minerals

MDPI

Article

Mineralogical and Geochemical Compositions of the Lopingian Coals in the Zhongliangshan Coalfield, Southwestern China

Jianhua Zou [1,2,*], Feng Han [1,2], Tian Li [1,2], Heming Tian [1,2] and Yingjiao Li [1,2]

1 Chongqing Key Laboratory of Exogenic Mineralization and Mine Environment, Chongqing Institute of Geology and Mineral Resources, Chongqing 400042, China; hanfeng01@sina.com (F.H.); lt_litian@163.com (T.L.); heming1986824@126.com (H.T.); Yingjiao_li@163.com (Y.L.)

2 Chongqing Reseach Center of State Key Laboratory of Coal Resources and Safe Mining, Chongqing 400042, China

* Correspondence: zoujianhua1200@gmail.com; Tel.: +86-023-8831-6044

Received: 10 January 2018; Accepted: 27 February 2018; Published: 6 March 2018

Abstract: The mineralogical and geochemical compositions of the Lopingian coals from an exploratory drill core (ZK4-1) in the Zhongliangshan Coalfield, southwestern China are reported in this paper. The Zhongliangshan coals are medium volatile bituminous in rank (random vitrinite reflectance, average 1.38%), characterized by a medium-ash yield (26.84%) and high sulfur content (3.38%). Minerals in the Zhongliangshan coals are mainly composed of clay assemblages (kaolinite, the illite/smectite mixed layer (I/S) and chamosite), pyrite, quartz, carbonate minerals (calcite, marcasite, ankerite, and dolomite), and anatase, followed by rutile, jarosite, natrojarosite, bassanite, gypsum and K-feldspar, with traces of apatite, rhabdophane and barite. Compared with the average concentrations of the world hard coals, some trace elements including Li, V, Co, Cu, Se, Y, Zr, Nb, rare earth elements (REE), Cd, Ta, Hf and Hg, are enriched in the Zhongliangshan coals. The modes of occurrence of chamosite, barite, rhabdophane, quartz and calcite in the Zhongliangshan coals indicate that the coals have probably been affected by the injection of low-temperature hydrothermal fluids. Based on the concentrations of Sc, V, Cr, Co, Ni, Cu and Zn, the ratios of Al_2O_3/TiO_2 and the upper continental crust-normalized rare earth element and yttrium (REY) distribution patterns of the Zhongliangshan coals, the dominant sediment source regions are the Leshan–Longnvsi Uplift, Hannan Upland, and Dabashan Uplift, with a small proportion of terrigenous materials from the Kangdian Upland. The K7 and the upper portion of K1 coals have the potential as raw materials for the recovery of REY.

Keywords: Lopingian coal; minerals; trace elements; Zhongliangshan Coalfield

1. Introduction

Studies on the trace elements of coal and non-coal horizons in coal-bearing sequences in southwestern China have attracted much attention, not only because some endemic diseases are related to coal utilization [1–5], but also because some critical elements (e.g., Ge, U, Ga, rare earth element and yttrium (REY)) are enriched in coal deposits [2,6–11].

The Zhongliangshan Coalfield, located in the eastern Sichuan Basin, is one of the main coal resource bases in Chongqing Municipality (Figure 1). Previous studies have shown that the dominant terrigenous material of the Lopingian coals in the Sichuan Basin is basaltic Kangdian Upland [12]. However, it has been reported recently that the dominant terrigenous materials for the Lopingian coals in the Huayingshan and Nantong coalfields, Sichuan basin are three Uplands/uplifts (TUUs), namely Leshan–Longnvsi Uplift, Dabashan Uplift and Hanan Upland rather than the Kangdian

Upland [8,13]. However, the sediment source region of the Lopingian coals in the Zhongliangshan Coalfield is not known. In addition, we have reported an anomalous enrichment of critical metals (Nb, Ga, and REY) in the tuff underlying the coal in the Zhongliangshan Coalfield, which can be regarded as a potential economically significant coal-bearing stratum hosting a polymetallic ore deposit [14,15]. The concentrations of rare metals in the Lopingian coals overlying the tuff layer need further investigation.

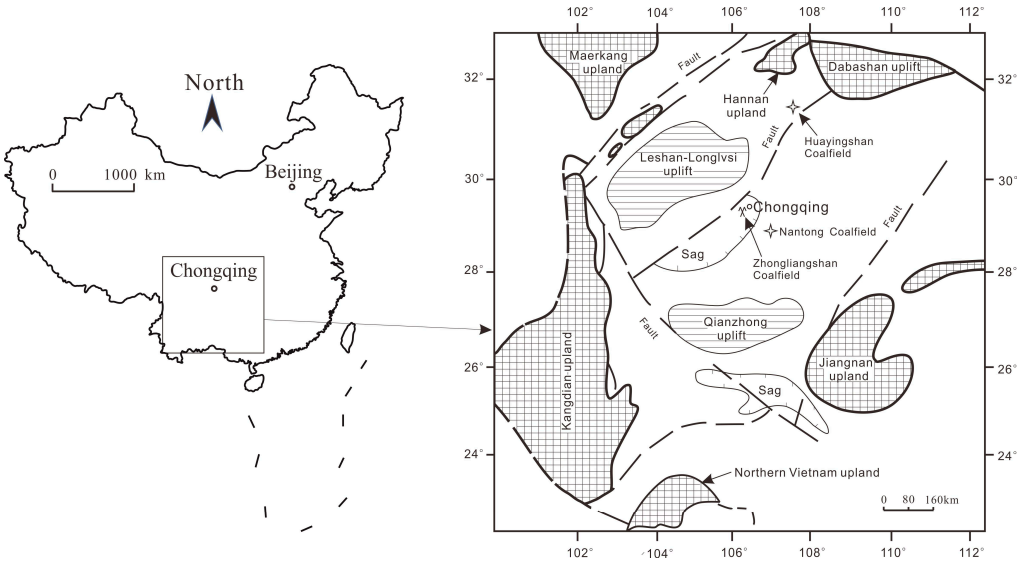

Figure 1. The location and tectonic map of the Zhongliangshan Coalfield.

The purpose of this paper is to address the sediment source region and to identify whether the Lopingian coals are enriched rare metals in the Zhongliangshan Coalfield based on the mineralogical and geochemical data.

2. Geological Setting

From bottom to top, the sedimentary sequences in the Zhongliangshan Coalfield are composed of the Middle Permian, Upper Permian, Lower Triassic, Middle Triassic, and Upper Triassic strata. The Middle Permian stratum is the Maokou Formation (P_2m), while the Upper Permian strata include the Longtan (P_3l) and Changxing Formations (P_3c). The Lower Triassic strata consisted of the Feixianguan (T_1f) and Jialingjiang Formations (T_1j). The Middle and Upper Triassic Formations are the Leikoupo Formation (T_2l) and Xujiahe Formation (T_3xj), respectively.

The Maokou Formation occurs as bioclastic limestone and displays light gray to dark gray, which underlies the Longtan Formation in disconformity. It has a thickness from 80 to 250 m (166 m on average).

The Longtan Formation is the coal-bearing stratum in the study area, and consists of the sandstone, siltstone, sandy mudstone, mudstone, and ten coal seams (indexed as K10 to K1 from bottom to top, Figure 2A). It is precipitated in a marine-continental transitional environment and has a thickness varying from 26.5 to 105.02 m (71.08 m on average). Some fossils are abundant in this formation, including brachiopods, fern and cephalopods.

The tuff layer is distributed widely in the lowermost Longtan Formaion in Chongqing. It has been discussed in detail, not only because the tuff is one of the marker beds in the coalfields [16] and can provide new evidence for the origin of the end-Guadalupian mass extinction [17], but also because the tuff can be considered as the potential sources for the critical elements [7,14]. The characteristics of the tuff layer in the study area have been described by Zou et al. [14].

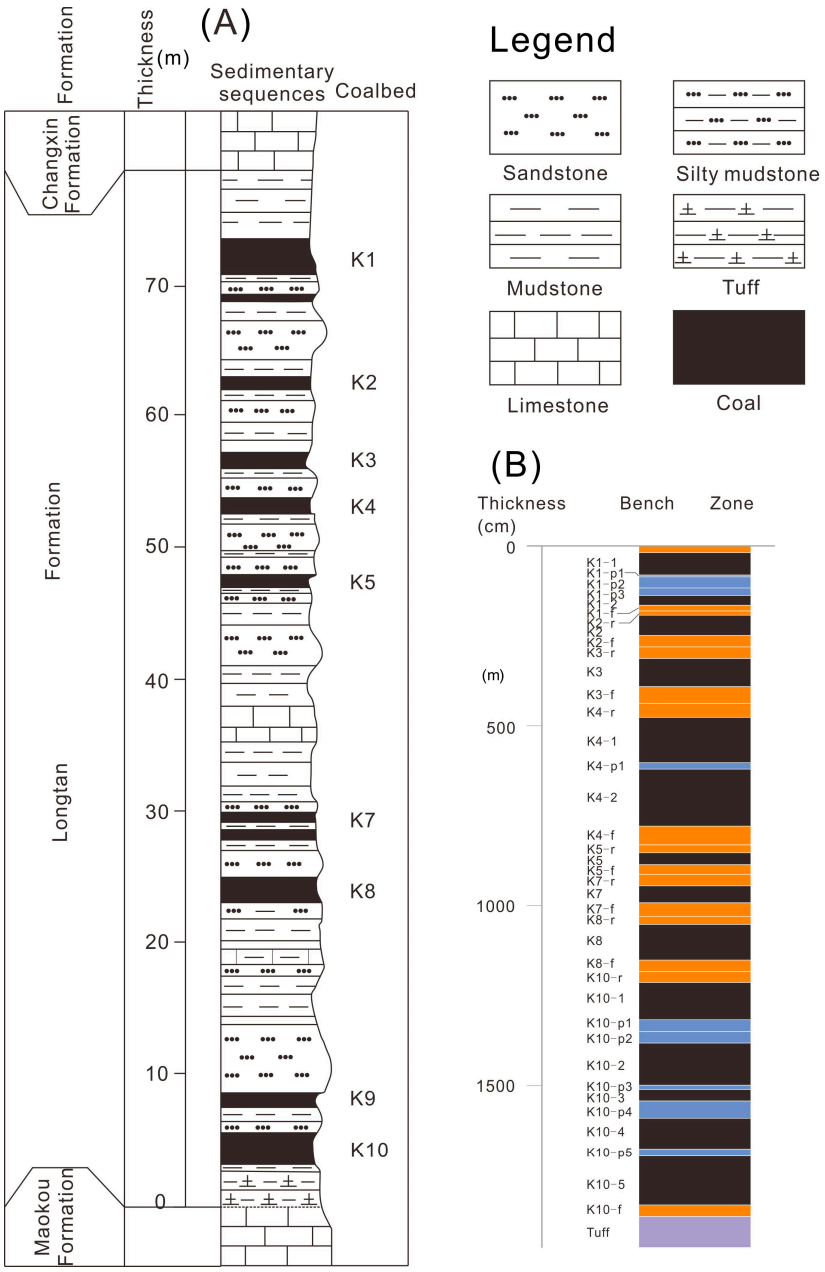

Figure 2. Sedimentary sequences of the Zhongliangshan Coalfield (**A**) and the collected samples of the ZK4-1 drill core in present study (**B**). Partings in blue, host rocks (roof and floor strata) in orange, tuff in purple, and coal benches in black. The suffixes r, f, and p stand for roof, floor, and partings, respectively.

The Changxing Formation, conformably overlying the Longtan Formation, consists of thick limestone intercalated with flint nodules and thin mudstone. It has a thickness of 102–114 m (108 m on average). This formation is enriched in brachiopods, spindle dragonflies, sponges, and other fossils.

Besides the Kangdian Upland, the Zhongliangshan Coalfield was surrounded by the Leshan-Longnvsi Uplift, Hannan Upland, and Dabashan Uplift (Figure 1) [8]. The Leshan-Longnvsi Uplift, Hannan Upland, and Dabashan Uplift were the vital positive structural units during the Lopingian stage, mainly composed of mudstone, sandstone and carbonate [18], could also provide the terrigenous materials for the coalfield during the coal-forming processes.

3. Sampling and Methods

A total of 40 samples of eight coal seams were taken from the exploratory drill core (No. ZK4-1) located in the Zhongliangshan Coalfield, Chongqing, southwestern China. These include 14 coal benches, nine partings, eight roofs, eight floors and one tuff samples (Figure 2B). Samples from each coal seam are numbered in an increasing order from top to bottom. The roof, partings, and floor strata were indexed with suffixes of r, p, and f, respectively. All samples were stored immediately in plastic bags to reduce oxidation and contamination. The Figure 2B shows the sample number, thickness, and lithology data in detail.

All the collected samples were treated through the procedures of air-drying, pulverizing, mixing and dividing using the method of coning and quartering. The coal samples were prepared with three types including <0.075 mm for geochemical analysis, <0.2 mm for proximate analysis, and <1 mm in size for petrographic analysis [19].

According to the ASTM Standards D3173-11, D3175-11, D3174-11 and D3177-02 [20–23], the proximate analysis and total sulfur were carried out. The forms of sulfur were tested based on the ASTM Standard D2492-02 [24]. The mean random reflectance of vitrinite (percent Ro, ran) was measured at a magnification of 500X using a Leica DM4500P microscope (Leica Inc., Wetzlar, Germany) in conjunction with a Craic QDI 302™ spectrophotometer (Craic Technologies, San Dimas, CA, USA). The gadolinium gallium garnet (Chinese Standard Reference GB13401) was used as the standard reference for vitrinite reflectance determination.

The mineralogical compositions of low-temperature ashing (LTA) of coal and non-coal samples were carried out using the powder X-ray diffraction (XRD). The instrument for the XRD analysis is D/max-2500/PC powder diffractometer (Rigaku Corporation, Tokyo, Japan). All the X-ray diffractograms of the coal LTAs and non-coal samples were subjected to quantitative mineralogical analysis using Siroquant™. The Siroquant™ is a commercial interpretation software, which is set out by Rietveld and developed by Taylor, respectively [25,26]. Ward et al. and Ruan and Ward have provided the utilization of this technique for coal-related materials in detail [27–29].

In order to study the microstructure and morphology of minerals, a scanning electron microscope (SEM, JSM-6610LV, JEOL, Tokyo, Japan) equipped with an energy-dispersive X-ray spectrometer (EDX, OXFORD X-max, Oxford Instruments, Abingdon-on-Thames, Britain) was used under the conditions of 20 kV accelerating voltage of and high vacuum mode.

The contents of carbon, hydrogen, and nitrogen in coal were determined using the elemental analyzer (VarioMACRO, Elementar, Langenselbold, Germany). Concentrations of major elements in the ashes (815 °C) were measured by X-ray fluorescence spectrometry (XRF, ARL ADVANTXP+).

Abundances of trace elements except for fluorine and mercury in all the samples were determined using the inductively coupled plasma mass spectrometry (ICP-MS, X series II, Thermo Fisher, Waltham, MA, USA). Before ICP-MS determination, an ultraClave microwave High Pressure Reactor (Milestone, Sorisole, BG, Italy)) was applied to digest the samples. Note that arsenic and selium were analyzed by ICP-MS with collision-cell technology (CCT) based on the method proposed by Li et al. [30]. The detailed ICP-MS procedures are discussed by Dai et al. [31,32]. Fluorine was analyzed using the method of pyrohydrolysis with an ion-selective electrode described in ASTM Standard D 5987-96 [33]. Mercury was determined using a Milestone DMA-80 Hg analyzer (Milestone, Sorisole, BG, Italy).

4. Results

4.1. Coal Characteristics

The proximate and ultimate analyses, total sulfur, forms of sulfur, and random vitrinite reflectance data for the 14 coal samples from the ZK4-1 drill core in the Zhonglianshan Coalfield are listed in Table 1. The average volatile matter and vitrinite reflectance are 25.77% and 1.38%, respectively, indicating a medium volatile bituminous coal based on the ASTM classification [34].

Based on the Chinese Standard GB/T 15224.1-2010 (coals with ash yield 10–20%, 20.01–30%, 30.01–40%, 40.01–50% are low-ash, medium-ash, medium and high-ash, high-ash coal, respectively), the K1, K4 and K10 are medium-ash coal; the K2 is low-ash coal; the K3 and K8 are medium and high-ash coal; and the K5 and K7 is high-ash coal. Based on the Chinese Standard GB/T 15224.2-2010 (coals with total sulfur content 1.01–2%, 2.01–3%, >3% are medium-sulfur, medium and high- sulfur, high-sulfur coal, respectively), the K1, K3 and K4 are medium-sulfur coal, the K2 is low-sulfur coal, and the K5, K7, K8 and K10 are all high-sulfur coals. The average total sulfur of present study is up to 3.38%, higher than that in the northeast India coals [35–37]. The sulfur in K1, K2, K7, K8 and K10 coals are mainly pyritic, however, sulfur in the K3, K4 and K5 is mainly organic.

Table 1. Proximate and ultimate analysis, forms of sulfur, and random vitrinite reflectance for coals from the ZK4-1 drill core in the Zhongliangshan Coalfield (%).

Sample	M_{ad}	A_d	V_{daf}	C_{daf}	H_{daf}	N_{daf}	$S_{t,d}$	$S_{p,d}$	$S_{s,d}$	$S_{o,d}$	$R_{o,ran}$
K1-1	1.13	18.13	23.67	88.63	5.3	1.73	1.89	1.56	0.09	0.24	1.34
K1-2	1.89	27.27	23.55	86.53	4.37	1.5	2.1	0.91	0.44	0.76	1.43
K1-av.	1.51	22.70	23.61	87.58	4.84	1.62	2.00	1.24	0.27	0.50	1.39
K2	1.66	17.19	23.67	88.5	4.66	1.56	2.18	1.14	0.14	0.9	1.39
K3	1.29	32.44	24.48	87.95	4.81	1.6	1.31	0.57	0.09	0.65	1.42
K4-1	1.1	21.38	27.66	90.12	4.78	1.69	1.17	0.36	0.05	0.76	1.37
K4-2	2.26	26.31	25.99	91.63	4.78	1.66	1.22	0.47	0.07	0.67	1.34
K4-av.	1.68	23.85	26.83	90.88	4.78	1.68	1.20	0.42	0.06	0.72	1.36
K5	1.36	52.56	31.09	72.25	4.69	1.08	11.8	4.29	0.67	6.84	1.35
K7	1.09	40.92	27.61	81.96	4.58	1.39	7.16	3.66	0.32	3.18	1.38
K8	2.17	30.83	26.76	86.26	4.75	1.52	3.13	2.11	0.16	0.87	1.37
K10-1	1.13	16.62	23.58	89.09	4.87	1.57	2.01	0.92	0.17	0.91	1.42
K10-2	2.97	20.77	22.97	89.49	4.37	1.49	1.98	0.58	0.52	0.88	1.31
K10-3	1.37	30.67	28.72	85.4	5.03	1.47	2.94	1.56	0.32	1.06	1.4
K10-4	1.67	20.91	26.23	86.83	4.81	1.5	4.72	2.3	0.67	1.74	1.4
K10-5	1.52	19.72	24.84	86.06	4.74	1.49	3.75	1.94	0.45	1.36	1.42
K10-av.	1.73	21.74	25.27	87.37	4.76	1.50	3.08	1.46	0.43	1.19	1.39
Average	1.61	26.84	25.77	86.48	4.75	1.52	3.38	1.6	0.3	1.49	1.38

M: moisture; A: ash yield; V: volatile matter; C: carbon; H: hydrogen; N: nitrogen; St: total sulfur; Sp: pyritic sulfur; So: organic sulfur; ad: air-dry basis; d: dry basis; daf: dry and ash-free basis; $R_{o,ran}$: random reflectance of vitrinite; av: average.

4.2. Mineralogical Characteristics in the Coals

Table 2 lists the the proportion of minerals in the coal LTAs, partings, roof and floor samples identified by X-ray diffractograms plus Siroquant. The minerals in the coal samples are composed mainly by kaolinite, quartz, pyrite, and calcite, with small proportions of anatase. I/S (mixed minerals of illite and smectite), chamosite, and dolomite are present in most of the samples. Marcasite, ankerite and siderite also occur in a few samples. Either jarosite or natrojarosite occurs in the LTAs of coals throughout the seam. The bassanite can be observed only in samples K1-1, K4-1 and K10-1, and the gypsum can be identified only in sample K2-1. K-feldspar is relatively abundant in the studied coals especially in sample K10-2, the proportion of which is up to 11.5% (ash basis). In addition, apatite, rhabdophane and barite have been identified under the SEM-EDX although they are below the detection limit of the XRD.

4.2.1. Kaolinite

From the K1 to K10, the proportion of kaolinite varies from 18.6% to 52.1% and averages 31.4% (LTA basis). Kaolinite in the coal occurs as cell-fillings in telinite and fusinite (Figure 3A–D). This is common in many other coals, and indicates formation by authigenic processes [38]. Vermicular kaolinite is also present (Figure 3B–D), a feature of which indicates an in-situ precipitation [39].

Table 2. Mineral compositions of coal LTAs and non-coal samples by X-ray diffraction (XRD) and Siroquant analysis (wt %).

Sample	LTA Yield	Quartz	Kaolinite	Illite	Illite/Smectite Mixed Layer	Chamosite	Anatase	Rutile	Pyrite	Marcasite	Calcite	Ankerite	Dolomite	Siderite	Jarosite	Natrojarosite	Barite	Bassanite	Gypsum	K-Feldspar	Albite
K1-1	20.74	11.2	27.5		22.8	3.6	1.9	0.8	7.9	2	17		1.8			1.6		1.9			
K1-2	30.90	31	31		12	3.9	2		7.2		5.2	0.7		0.1		2.3				4.6	
K2	20.29	16.2	30.5		21.1	1.1	2.2	0.4	11.8	1.5	8		0.9			2.3			4		
K3	37.27	26.2	22.8		31.4		2.3		2.7		7.5	1.1		0.2		1.3				4.5	
K4-1	24.52	21.6	23.2		22	1.4	1		4.4	2.1	18.6		1.3			2		2.6			
K4-2	29.46	11	36.2		21.5	5.4	2.9		3.2		15.9		1.5		0.7					1.8	
K5	63.69	45.3	18.6				1.7		18.4	4.8	2.2		0.8			2.7				5.5	
K7	47.93	29.5	32.5		5.3	3.9	1.3		13.8	1.4	6.9		2.5		1.6					1.5	
K8	35.41	20.9	34.1		24.2		2.2		7		8.1		0.6			0.7				2.2	
K10-1	19.59	17.3	38.1			5	2.7		9.6		21.1		1.1			2.5		2.6			
K10-2	24.35	20.2	39.3			2.3	3.7		10.9		6.2					5.8				11.5	
K10-3	35.71	6.8	52.1		15.9		1.6		10.4		9.9		1.5			1.8					
K10-4	26.21	10.2	30.1		16.9	1.4	2		19.7		13.7		0.9			5.1					
K10-5	24.12	12.6	28		18.5	1.9	2.5		20.4		10.9		0.9			4.4					
K1-r	nd	24.1	6.1		42.7		2.1		13.4		0.5			0.5						4.5	5.9
K1-p1	nd	7.4	47		32.1		5.8		1.5					0.2						3.3	2.7
K1-p2	nd	13.3	31.2		30		3.5		2.2		0.5			9.2						4.8	5.2
K1-p3	nd	5.4	23		44.1		3.6		1.2					3.5						7.1	12.1
K1-f	nd	13.8	18.5		37.2		3.5		2.1		0.3			15.8						3.9	4.9
K2-r	nd	21.8	4.7	5.4	41.7		2.3		13.9			2.9							1		6.4
K2-f	nd	14.8	1.4		31.7		3.2		2.7		3.6	1.3		22.4						8.1	10.8
K3-r	nd	12.3	14		48.3		3		9.3		0.4			0.3						4.5	7.9
K3-f	nd	11.2	4.9		62.5		2.7		2.8		0.6	1.2		0.9					1.4	6.6	5.1
K4-r	nd	9.3	13.3		46.5		3.7		0.3		0.6	1.8		9.3							15.2
K4-p1	nd	9.6	17.6		51.4		3.3		8.9										1.9		7.4
K4-f	nd	6.7	52.2		29.1		5.1		2.3		0.4			4.2							
K5-r	nd	14.4	20.2		38.2		1.8		16.1		0.5					3.1				5.7	
K5-f	nd	12.1	27.5		42.3		4.3		4.3		0.2			5.1						4.2	
K7-r	nd	3.7	52.8				3.6		1					32.9						6.1	
K7-f	nd	4.3	54.5		25.1		4.7		0.7		0.5			6.6						3.4	
K8-r	nd	1.8	34.3		38.2		2.3		1.5		3.6			13							5.3
K8-f	nd	7.6	20		52.9		4.1		4		1			5.1		0.9			1.2		3.3
K10-r	nd	6.8	37.7		35.4		2.7		6.3		0.9	0.5		2.4		0.7					6.7
K10-p1	nd	4.9	36.6		34.9		2.7		9.9					1.1		1.2			2.3		6.5
K10-p2	nd	4.9	39.5		29.8		2.3		15.7				0.3	0.2		1.6				5.7	
K10-p3	nd	6.2	42.5		23.8		3.6		6.7		4		0.4	4.8		0.3			2.7	5	
K10-p4	nd	2	40.6		23.3		1.7		22.6		2.1					1.6			2.3	3.8	
K10-p5	nd	4.2	15				0.9		29.5		40.7				1.8		2.1		5.7		
K10-f	nd	2.3	20.6		32.9	2.8	1.6		9.1		5.7			20							4.9
Tuff	nd		28.6	14.1			2.4		21.1		33.8										

nd: no data.

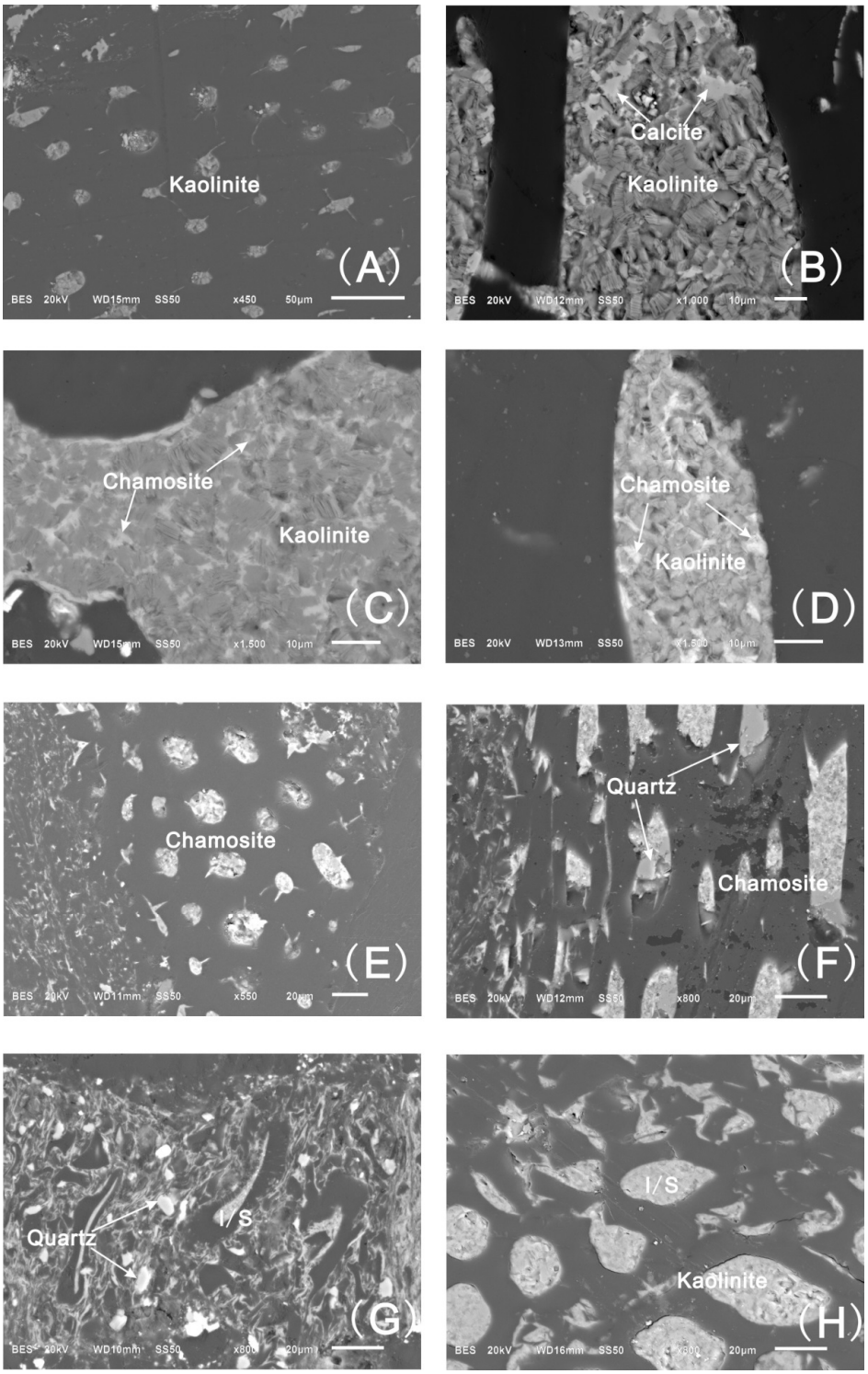

Figure 3. Scanning electron microscope (SEM) back-scattering images of minerals in the Zhongliangshan coals. (**A**) cell-filling kaolinite in sample K8-1; (**B**) cell-filling kaolinite and calcite in sample K1-1; (**C**) cell-filling kaolinite and chamosite in sample K5-1; (**D**) cell-filling kaolinite and chamosite in sample K5-2; (**E**) cell-filling chamosite in sample K4-2; (**F**) cell-filling chamosite and quartz in sample K10-5; (**G**) I/S and quartz occurred in the matrix in sample K10-4. (H) cell-filling I/S and kaolinite in sample K4-1.

4.2.2. Chamosite

Two species of chlorite could occur in coal (chamosite and clinochlore), although it is not commonly observed in coal. Chamosite and clinochlore have the same diffraction peaks in the XRD patterns and can be identified by their different intensities of peaks in X-ray diffractograms [40,41]. The chlorite present in this study was identified as chamosite rather than clinochlore, not only because of the weaker odd-order peaks (001 and 003) of XRD patterns but also because of high Fe and low Mg percentages determined by the energy dispersive X-ray (EDX) analysis.

XRD studies indicate that chamosite occurs in all of the coal LTA residues except for the coal samples K3, K5 and K8. The chamosite, usually coexisting with the kaolinite (Figure 3C,D), occurs as cell-fillings in the coal (Figure 3C–F), indicating an authigenic origin.

4.2.3. Illite/Smectite Mixed Layer

The Zhongliangshan coals have significant proportions of illite/smectite mixed layer (I/S) (Table 2). The I/S in the coal is filled in the plant matrix (Figure 3G) or in the cell cavity (Figure 3H), indicating that the I/S in present study is of authigenic origin.

4.2.4. Pyrite

Pyrite is a common mineral in the Lopingian coal seams in southwestern China [8,39,42–44]. From the K1 to K10 coal LTA residues, the proportion of pyrite increases gradually, from 2.7% (K3-1) to 20.4% (K10-5) and with an average of 10.5%. The pyrite in the samples occurs as euhedral crystals (Figure 4A,B), and as replacement of the maceral components (Figure 4C).

4.2.5. Quartz

Quartz in the coal LTA residues varies from 6.8% to 45.3% and averages 20%. Quartz occurs as cell infillings and euhedral crystal (Figure 4D–F), indicating an authigenic origin.

4.2.6. Calcite, Ankerite, Dolomite, and Siderite

Calcite is abundant in the Zhongliangshan coals, varying from 2.2% to 21.1% and with an average of 10.4%. The dolomite was detected in all the coal LTA residues except samples K1-2, K3-1 and K10-2. However, the ankerite and siderite were identified only in samples K1-2 and K3-1. Calcite occurs as cell-fillings (Figure 4G,H) and fracture-fillings (Figure 5A), indicating an epigenetic origin. The mode of occurrence of ankerite is similar to that of calcite (Figure 5B,C), indicating that it has an epigenetic origin as well.

4.2.7. Anatase

Anatase is present commonly in the Lopingian coals in southwestern China, mainly derived from the sediment source region from high-Ti basalt in the Kangdian upland and injection of hydrothermal solutions [8,45]. Anatase is distributed in all the coal LTA residues, and varies from 1% to 3.7% in abundance (2.1% on average). Anatase occurs as a replacement of glass shards or pumice (Figure 5D), similar to that in the K2 coal in the Songzao coalfield [39].

4.2.8. Apatite, Barite and Rhabdophane

Apatite in the Zhongliangshan coals is distributed in the collodetrinte (Figure 5E). Barite occurs as cavity-fillings, indicating an authigenic origin (Figure 5F). Rhabdophane appears to be as cell-fillings associating with kaolinite and chamosite (Figure 5G,H).

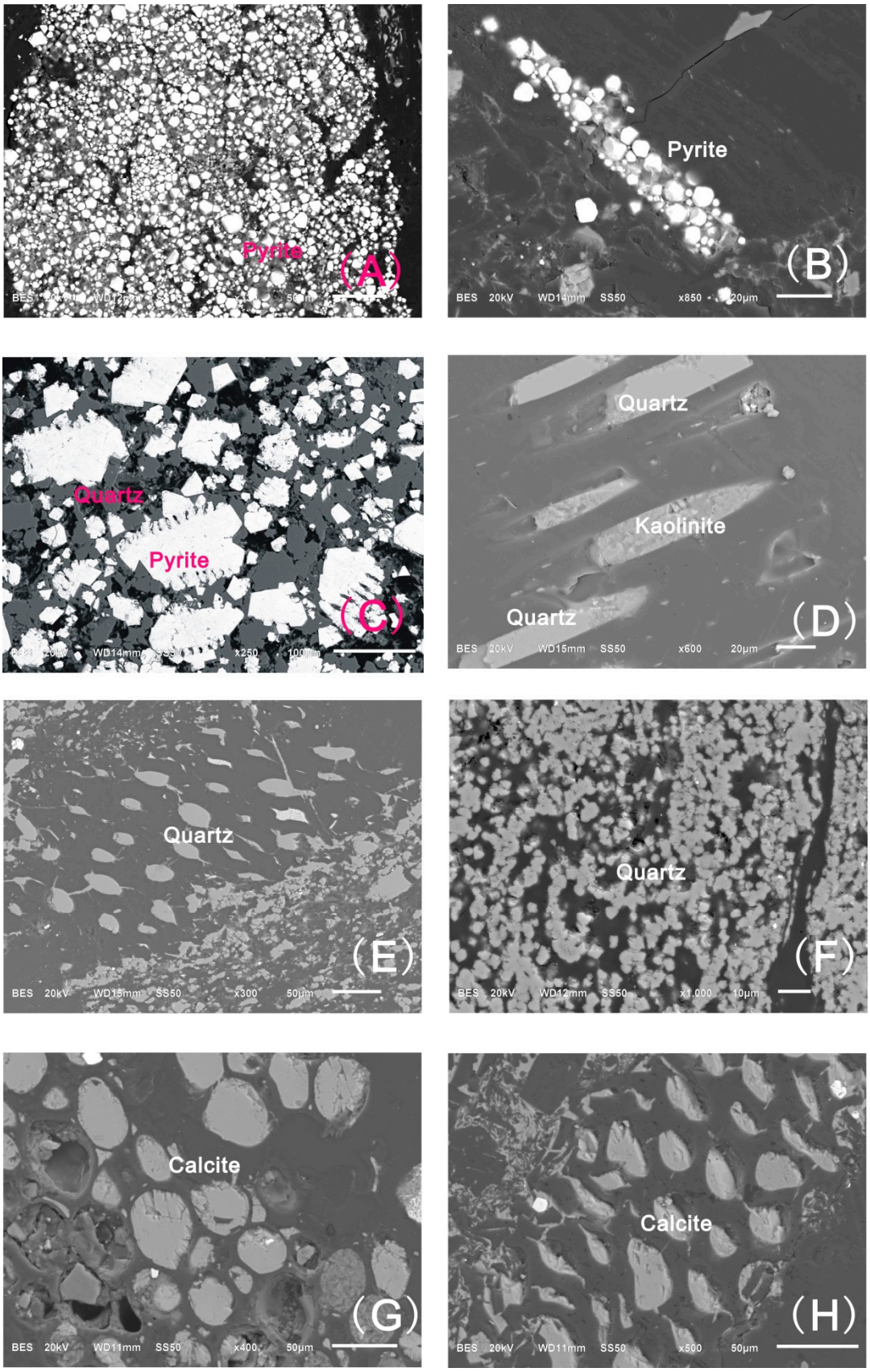

Figure 4. SEM back scattering images of minerals in the Zhongliangshan coals. (**A**) euhedral pyrite in sample K1-1; (**B**) euhedral pyrite in sample K10-4; (**C**) pyrite in sample K7-1; (**D**) cell-filling quartz and kaolinite in sample K1-2; (**E**) cell-filling quartz in sample K5-1; (**F**) quartz in sample K4-2; (**G**) cell-filling calcite in sample K4-2; (**H**) cell-filling calcite sample K4-2.

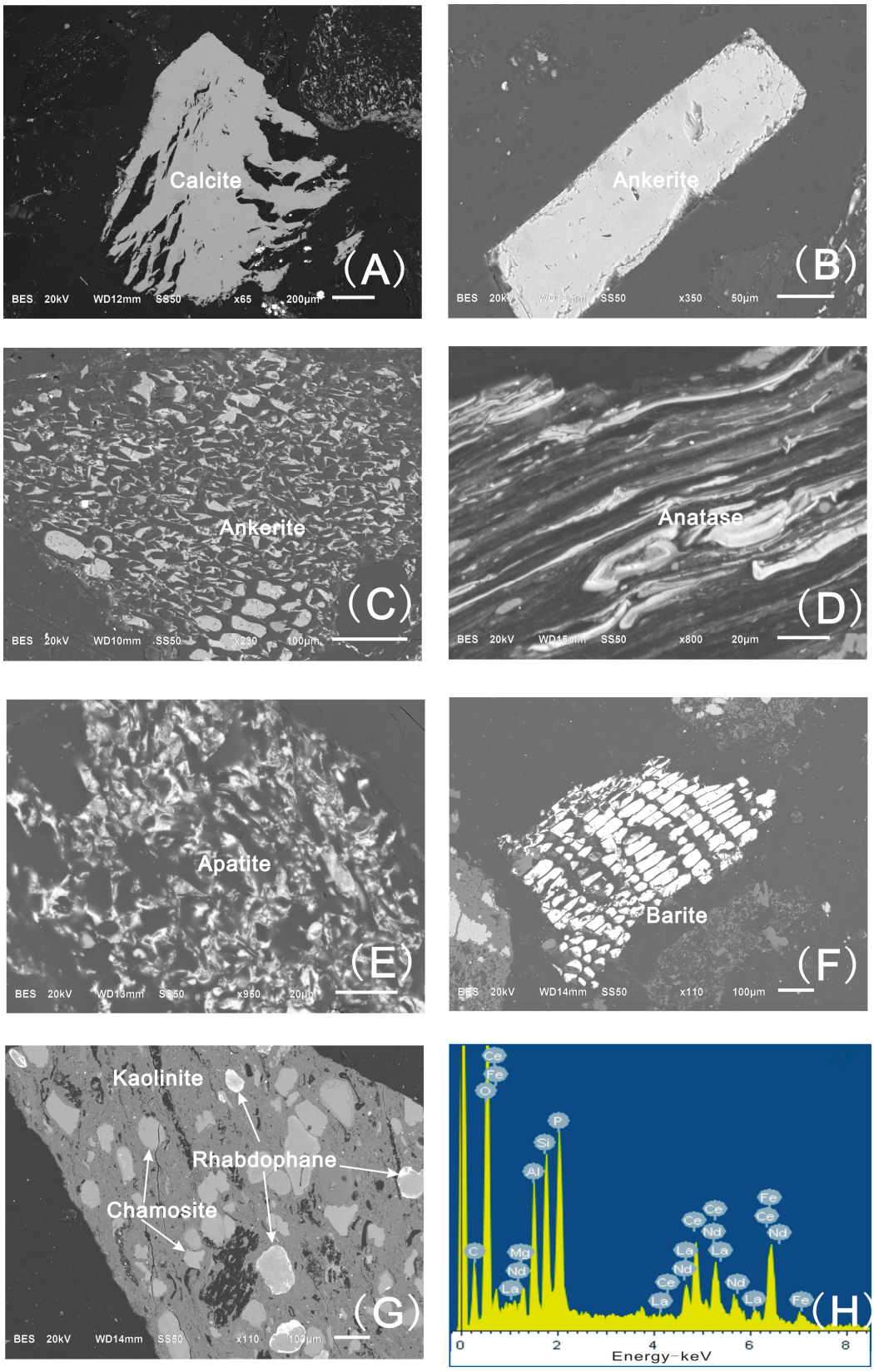

Figure 5. SEM back scattering images of minerals in the Zhongliangshan coals. (**A**) fracture-filling calcite in sample K1-1; (**B**) cell-filling ankerite in sample K1-1; (**C**) cell-filling ankerite in sample K10-4; (**D**) anatase occurring as replacement of glass shards or pumice in sample K4-2; (**E**) apatite distributed in the collodetrinte in sample K10-3; (**F**) barite occurring as cavitiy-fillings in sample K7-1; (**G**) rhabdophane, kaolinite and chamosite in sample K7-1; (**H**) the energy dispersive X-ray (EDX) spectrum of rhabdophane in sample K7-1.

4.3. Geochemical Characteristics

4.3.1. Major Elements

The major elements in the Zhongliangshan coals are dominated by SiO_2 and Al_2O_3, and to a lesser extent, Fe_2O_3 and CaO (Table 3). In comparison with Chinese coals [2], the concentrations of SiO_2, TiO_2 and MgO in studied coals are slightly higher. However, the abundances of other major element oxides are lower than those in Chinese coals. The SiO_2/Al_2O_3 ratio (2.24) of the Zhongliangshan coals is higher than the average Chinese coals (1.42) [2].

4.3.2. Comparison between Mineralogical and Chemical Compositions

Based on the calculation methods described by Ward et al. [27], the reliability of the quantitative XRD data was checked by the comparison with the observed ash chemistry determined by XRF. Before the comparison, data from the two methods were both normalized to allow for difference in LTA, CO_2, H_2O^+, and SO_3 percentages [46]. The correlations of SiO_2, Al_2O_3, K_2O, Fe_2O_3, TiO_2, CaO and MgO are revealed in Figure 6.

For SiO_2, Al_2O_3, Fe_2O_3 and TiO_2, the points fall very close to the diagonal equality line, indicating that the minerals indicated by the XRD analysis are highly consistent with the independently-determined chemical data. The plots for CaO and MgO show that the data points of CaO tend to fall above the equality line and that of MgO fall below the equality line, indicating that partial Ca^{2+} was replaced by Mg^{2+} in the calcite, this is also observed by the SEM-EDX analysis. The plot for Na_2O also shows that the points are close to the equality line. However, the points of K_2O fall below the diagonal equality line, implying the I/S may have a lesser K^+.

4.3.3. Trace Elements

From the Table 3 and Figure 7, it can be obtained that some trace elements are enriched in comparison with the average concentrations of the world hard coals [47]. The concentration coefficients (CC, the ratio of the trace-element concentrations in investigated samples vs. world hard coals) [32] of trace elements between 5 and 10 include Se, Zr, Nb, Cd and Ta. Many other elements in the coals (Li, V, Co, Cu, Hf and Hg) are slightly enriched (2<CC<5). Elements B, As, Rb, Sb, Tl and Bi are depleted, with a CC <0.5. The remaining trace elements have concentrations close to the world hard coals, with CC between 0.5 and 2.

Sc, V, Cr, Co, Ni, Cu and Zn

It is worthy to note that Sc, V, Cr, Co, Ni, Cu and Zn, which are significantly abundant in the basalt of Kangdian Upland [11,43,45,48,49], are not highly enriched in the Zhongliangshan coals. Compared with the Lopingian C2 and C3 coals in the Xinde Mine (Yunnan Province, China) [45], with the sediment-source region of the Kangdian Upland, concentrations of Sc, V, Cr, Co, Ni, Cu and Zn of present study are relatively lower (Figure 8). However, concentrations of Sc, V, Cr, Co, Ni, Cu and Zn of the Zhongliangshan coals are relatively higher than those of the Lopingian coals in the Donglin Mine and Lvshuidong Mine (Figure 8) [8,13], with the dominant sediment source regions of the Leshan-Longnvsi Uplift, Hannan Upland, and Dabashan Uplift rather than the Kangdian Upland.

Rare Earth Elements and Yttrium

Although there are some inconsistencies on the abbreviation of "REE" or "REY" in some geochemical literature [50], REY is adopted in this study to represent the lanthanides and Yttrium [51]. Owing to the unique geochemical behaviors, REY have been widely used as geochemical parameters to identify sediment source region and clarify the evolution processes of coal basins [51–59].

Table 3. Major element oxides (%) and trace elements in the coal and non-coal samples from the ZK4-1 drill core in the Zhongliangshan Coalfield (μg/g).

Sample	SiO_2	TiO_2	Al_2O_3	Fe_2O_3	MnO	MgO	CaO	Na_2O	K_2O	P_2O_5	SiO_2/Al_2O_3	Li	Be	B	F	Sc	V	Cr	Co	Ni	Cu	Zn
K1-1	7.98	0.27	4.54	2.29	0.009	0.28	1.15	0.086	0.132	0.022	1.76	35.5	2.85	21	84. 5	4.53	49.7	17.3	15.2	21.5	37.9	95.9
K1-2	14.98	0.45	5.99	3.06	0.016	0.32	0.63	0.143	0.305	0.025	2.50	44.7	3.16	24.7	100	5.86	60	27.6	12.6	21.8	46.3	32.1
K1-av.	11.48	0.36	5.27	2.68	0.01	0.30	0.89	0.11	0.22	0.02	2.13	40.05	3	22.9	92.3	5.2	54.8	22.5	13.9	21.6	42.1	64
K2	7.81	0.34	4.16	2.46	0.008	0.21	0.72	0.075	0.132	0.021	1.88	36.6	2.63	17.8	42.7	4.02	41.6	20.6	9.45	12.5	24.4	17.1
K3	17.76	1.02	7.24	2.42	0.012	0.39	1.24	0.182	0.378	0.021	2.45	49.7	4.37	30.6	95.7	7.16	96.7	40.4	10.7	42.1	45.2	21.2
K4-1	10.59	0.35	4.49	1.79	0.012	0.26	1.54	0.118	0.166	0.018	2.36	32.1	2.12	14	48.3	4.64	48.1	20.1	13.3	22	30.8	25.1
K4-2	12.00	0.76	6.92	2.47	0.013	0.32	1.37	0.182	0.164	0.024	1.73	50.3	2.95	17.5	62	8.05	108	35.1	14.6	25.6	89.2	41.1
K4-av.	11.29	0.55	5.70	2.13	0.01	0.29	1.45	0.15	0.16	0.02	2.05	41.2	2.54	15.7	55.1	6.35	78.1	27.6	13.9	23.8	60	33.1
K5	29.22	0.54	6.24	13.10	0.014	0.48	0.72	0.213	0.143	0.024	4.68	30	3.38	19.5	63.1	7.65	71.7	38.1	15.9	40.3	41.8	39
K7	20.62	0.54	6.64	9.06	0.018	0.35	1.06	0.14	0.136	0.041	3.11	37	7.37	18.7	70.2	8.6	129	30.1	35.9	58.9	84	226
K8	14.96	0.76	7.37	4.14	0.013	0.23	0.93	0.171	0.268	0.025	2.03	36.8	4.4	38.1	178	7.44	79.2	33.6	17.7	28	42.7	26.7
K10-1	7.10	0.26	3.93	2.48	0.008	0.23	1.09	0.066	0.117	0.015	1.80	34.7	3.14	22.4	72.3	4.32	42.7	17.3	8.7	12.3	33.5	20
K10-2	9.48	0.39	4.83	2.85	0.01	0.28	0.82	0.138	0.238	0.027	1.96	35.1	3.09	23.7	111	4.48	42.8	19.2	7.52	13.2	28.9	27.6
K10-3	12.90	0.70	8.53	3.80	0.022	0.27	1.64	0.107	0.15	0.051	1.51	57.3	3.86	36.4	160	5.91	67.3	27.5	11.1	20.8	40.2	17.7
K10-4	7.39	0.27	4.17	5.17	0.009	0.22	1.31	0.083	0.111	0.076	1.77	35.5	2.74	16.6	96.3	5	58.4	22	8.81	18.9	30.9	14
K10-5	7.58	0.25	4.07	4.43	0.009	0.23	1.14	0.070	0.117	0.053	1.86	38.4	2.92	19.5	78.4	4.91	56.6	19.1	8.64	16.8	27.6	10.9
K10-av.	8.89	0.37	5.11	3.74	0.01	0.25	1.20	0.09	0.15	0.04	1.78	40.2	3.15	23.7	104	4.93	53.6	21	8.96	16.4	32.2	18
All coals-av.	12.88	0.49	5.65	4.25	0.01	0.29	1.10	0.13	0.18	0.03	2.24	39.6	3.5	22.9	90.2	5.9	68	26.3	13.6	25.3	43.1	43.9
China	8.47	0.33	5.98	4.85	0.015	0.22	1.23	0.16	0.19	0.092	1.42	31.8	2.11	53	130	4.38	35.1	15.4	7.08	13.7	17.5	41.4
World	nd	0.148	nd	nd	0.011	nd	nd	nd	nd	0.057	nd	14	2	47	82	3.7	28	17	6	17	16	28
K1-r	52.71	2.32	16.91	8.97	0.079	0.85	0.89	0.984	2.141	0.238	3.12	21	2.78	126	667	22.5	251	93.3	33.8	67.3	133	107
K1-p1	41.79	6.04	25.99	3.78	0.005	0.62	0.29	0.576	0.872	0.055	1.61	162	3.42	102	246	28.8	417	262	48.5	113	220	106
K1-p2	33.75	2.43	18.60	11.91	0.21	1.05	1.49	0.728	0.779	0.306	1.81	73.5	3.03	76.4	655	22.8	246	124	49.5	84	131	157
K1-p3	42.82	3.96	24.60	7.47	0.092	1.23	0.76	1.288	1.39	0.134	1.74	95.2	2.96	125	397	30.3	394	257	48	93.2	162	200
K1-f	37.36	3.01	19.17	12.83	0.157	1.07	0.77	0.798	1.062	0.075	1.95	67.4	2.64	81.6	292	24.4	274	154	51.6	81.7	128	147
K2-r	50.41	2.51	16.82	9.95	0.045	1.21	1.18	0.966	2.333	0.131	3.00	16.8	3.67	148	538	25.6	329	161	66.9	102	123	152
K2-f	38.86	2.76	15.50	18.46	0.192	1.47	2.16	1.382	1.058	0.243	2.51	36.9	1.96	64.2	489	17.9	286	194	40.3	78.8	110	120
K3-r	43.86	2.57	20.02	9.28	0.064	1.1	0.92	1.278	2.086	0.279	2.19	62	3.31	117	759	23.9	370	125	55.9	112.8	163	160
K3-f	45.25	5.11	21.66	5.85	0.035	1.08	0.80	0.948	3.117	0.11	2.09	30.6	3.82	159	654	27.9	393	191	42.7	96.6	206	150
K4-r	40.07	3.63	20.32	11.64	0.22	1.38	1.50	1.335	1.813	0.285	1.97	41.9	2.92	100	607	17.4	307	168	33.9	70	185	176
K4-p1	38.71	2.52	20.04	7.60	0.121	1	0.55	0.841	1.928	0.138	1.93	83.7	4.1	116	523	27.5	369	124	53.1	66.5	155	150
K4-f	40.24	4.48	25.93	8.01	0.037	0.79	0.35	0.684	0.558	0.064	1.55	125	5.35	94.8	284	9.97	430	178	75.9	108	216	119
K5-r	41.95	1.53	19.63	13.05	0.009	0.89	0.27	0.958	1.127	0.111	2.14	65.2	5.55	126	330	16.5	198	83.7	37.2	50.1	69.9	268
K5-f	40.43	3.93	21.71	10.46	0.072	0.9	0.37	0.977	0.969	0.056	1.86	86.2	3.73	129	362	29.9	358	191	55.4	105	209	150
K7-r	27.92	2.82	19.79	22.56	0.58	1.44	0.73	0.548	0.247	0.158	1.41	113	13.9	56.8	375	16.5	229	82.6	51.2	50.4	107	370
K7-f	36.56	4.29	24.93	9.32	0.132	0.58	0.60	0.56	0.653	0.086	1.47	126	6.97	105	398	11.2	321	186	33.4	58.8	219	155
K8-r	36.21	2.37	25.03	13.62	0.157	0.86	1.13	0.907	1.198	0.066	1.45	91.7	4	128	468	8.52	377	226	60	113	112	166
K8-f	36.74	3.32	21.20	11.22	0.135	0.84	0.69	0.689	2.102	0.076	1.73	49.8	5.76	145	932	15	265	153	48.3	83.1	142	161
K10-r	38.57	2.24	25.26	11.20	0.055	0.83	1.68	0.828	1.49	0.547	1.53	73	4.22	127	1167	21.7	295	172	42.8	93.1	94.7	191
K10-p1	36.37	2.43	24.65	11.01	0.007	0.49	1.41	0.712	1.378	0.721	1.48	72.3	3.25	122	1254	26.6	301	260	45.5	115	122	184
K10-p2	33.42	2.04	23.35	16.56	0.018	0.46	0.87	0.738	1.158	0.39	1.43	82.4	3.25	106	957	20.7	254	193	43.8	79.9	96.9	191
K10-p3	31.56	2.95	20.64	11.46	0.103	0.7	1.75	0.518	0.448	0.073	1.53	115.6	6.12	83.4	358	22.8	291	113	44	72.1	142	78.2
K10-p4	28.67	1.61	22.29	20.76	0.032	0.35	1.05	0.478	0.685	0.086	1.29	84.1	4.1	82.2	497	10.3	258	193	37.9	81.8	87.7	146
K10-p5	8.17	0.39	5.89	27.25	0.037	0.18	8.10	0.074	0.115	0.018	1.39	24.8	0.77	10.8	90.6	7.37	103	85.4	26.8	94	49.2	45.9
K10-f	33.42	2.11	23.14	16.27	0.09	1.27	2.61	0.777	1.376	0.144	1.44	70.4	3.2	105	729	18.7	263	223	44.4	87.3	83.2	156
Tuff	21.40	3.12	18.53	16.39	0.036	0.27	11.81	0.095	0.421	0.021	1.16	176	3.04	71.6	379	17.1	414	176	29.6	105	128	44.6

Sample	Ga	Ge	As	Se	Rb	Sr	Zr	Nb	Mo	Cd	In	Sn	Sb	Cs	Ba	Hf	Ta	W	Hg	Tl	Pb	Bi	Th	U
K1-1	7.87	3.51	1.57	8.09	3.54	183	173	19	2.2	0.64	0.08	2	0.39	1.83	26	4.12	1.87	1.35	0.41	bdl	11.1	0.28	5.69	3.33

Table 3. *Cont.*

Sample	SiO_2	TiO_2	Al_2O_3	Fe_2O_3	MnO	MgO	CaO	Na_2O	K_2O	P_2O_5	SiO_2/Al_2O_3	Li	Be	B	F	Sc	V	Cr	Co	Ni	Cu	Zn		
K1-2	9.91	3.25	2.36	8.36	9.23	141	183	25.5	1.33	0.32	0.07	2.38	0.23	1.58	58.6	4.49	1.78	2.47	0.23	0.04	14.3	0.24	6.22	2.57
K1-av.	8.89	3.38	1.96	8.22	6.38	162	178	22.2	1.77	0.48	0.07	2.19	0.31	1.70	42.3	4.3	1.83	1.91	0.32	0.04	12.7	0.26	5.95	2.95
K2	8.26	4.19	3.27	7.44	3.17	142	158	20.4	1.21	0.26	0.06	1.67	0.25	0.43	29.2	3.9	1.39	1.26	0.24	0.01	10.9	0.24	5.28	2.74
K3	11.3	2.36	1.53	8.63	9.4	226	253	42.6	2.66	0.37	0.08	3.08	0.86	2.84	107	6.35	3.22	2.41	0.26	0.15	20.1	0.29	8.69	2.5
K4-1	7.44	3.5	0.62	4.54	3.7	174	98.9	13.2	0.92	0.26	0.05	1.48	0.17	1.47	55.5	2.68	0.93	1.03	0.15	bdl	9.58	0.22	4.6	1.78
K4-2	12.2	3.22	2.08	8.21	3.79	243	185	25.2	1.22	0.61	0.07	2.37	0.33	0.82	119	4.78	1.83	1.88	0.13	bdl	12.1	0.23	6.39	2.05
K4-av.	9.83	3.36	1.35	6.38	3.75	209	142	19.2	1.07	0.43	0.06	1.92	0.25	1.14	87	3.73	1.38	1.46	0.14	bdl	10.8	0.22	5.5	1.91
K5	7.68	1.31	4.78	10	2.63	162	253	29.7	12.2	0.48	0.05	1.25	0.28	bdl	44.7	3.33	0.54	6.57	1.16	0.14	15.8	0.15	3.96	2.21
K7	11.8	2.53	9.06	8.36	2.7	215	351	24.9	4.25	1.95	0.07	2.67	0.46	0.56	857	6.72	0.94	4.65	0.57	0.07	37.9	0.2	8.65	2.58
K8	11.7	2.98	2.38	9.34	4.18	172	299	41.9	2.44	0.45	0.09	2.96	0.23	1.32	253	7.2	2.67	2.02	0.46	bdl	12	0.24	9.35	2.8
K10-1	7.03	3.8	1.64	8.39	1.63	142	113	4.61	0.35	0.22	0.06	1.64	0.1	0.46	139	2.92	bdl	0.21	0.23	bdl	8.74	0.22	4.82	2.69
K10-2	9.41	2.9	1.59	5.38	5.74	133	225	27.2	1.2	0.42	0.08	2.07	0.12	1.21	206	5.62	1.62	0.72	0.22	0.02	10.8	0.27	7.05	2.73
K10-3	15.6	3.29	3.45	8.88	5.07	188	366	63.6	2.16	0.54	0.13	3.7	0.28	bdl	244	10.3	5.61	1.72	0.72	0.1	11.1	0.35	13.4	4.66
K10-4	6.52	3.1	3.5	7.96	2.41	259	92.3	10.9	1.92	0.21	0.04	1.25	0.09	bdl	640	2.38	0.73	0.75	0.7	0.05	7.14	0.21	4.03	2.1
K10-5	6.61	3.08	2.05	6.74	2.26	219	87.8	9.95	1.52	0.18	0.05	1.22	0.09	bdl	366	2.32	0.53	0.16	0.49	0.01	6.94	0.21	4.05	2.31
K10-av.	9.03	3.23	2.45	7.47	3.42	189	177	23.3	1.43	0.31	0.07	1.98	0.14	0.83	319	4.71	2.12	0.71	0.47	0.04	8.95	0.25	6.67	2.9
All coals-av.	9.52	3.07	2.85	7.88	4.25	186	203	25.6	2.54	0.49	0.07	2.12	0.28	1.25	225	4.8	1.68	1.94	0.43	0.07	13.5	0.24	6.58	2.65
China	6.55	2.78	3.79	2.47	9.25	140	89.5	9.44	3.08	0.25	0.05	2.11	0.84	1.13	159	3.71	0.62	1.08	0.16	0.47	15.1	0.79	5.84	2.43
World	6	2.4	8.3	1.3	18	100	36	4	2.1	0.20	0.04	1.4	1.00	1.10	150.00	1.20	0.30	0.99	0.10	0.58	9.00	1.10	3.20	1.90
K1-r	25.8	1.52	27.7	3.76	44.6	604	366	46.5	1.3	0.59	0.12	3.66	0.31	6.17	208	9.29	3.33	3.03	0.19	0.28	13.3	0.14	9.64	5.02
K1-p1	40	3.1	5.07	2.79	11.5	375	669	97.4	2.84	1	0.2	5.50	0.11	1.86	139	16.5	7.77	5.91	0.11	0.04	22.8	0.14	10.6	6.86
K1-p2	23.4	1.96	6.56	3.13	16	443	359	47.3	1.05	0.65	0.11	3.09	bdl	0.41	164	8.28	3.8	2.97	0.09	0.04	13.4	0.08	8.26	2.45
K1-p3	36.1	2.09	5.33	1.56	23.8	595	419	60.2	1.28	0.75	0.14	3.76	bdl	5.13	238	10.4	5.2	1.66	0.02	0.03	10.4	0.08	9.17	2.62
K1-f	26.6	1.89	5.62	3.02	24.1	432	415	59.7	1.3	0.87	0.12	3.39	0.01	2.3	211	9.84	4.51	2.11	0.07	0.04	12.3	0.08	9.39	3.29
K2-r	26.9	2.09	27.3	5.11	65.1	549	367	42.9	3.57	0.63	0.11	3.16	0.38	2.68	299	8.7	3.26	1.62	0.12	0.21	17.6	0.15	8.48	11.7
K2-f	21.3	1.85	7.11	3.17	25.9	626	343	35.2	0.82	0.54	0.1	2.54	bdl	0.71	227	7.74	1.91	1.34	0.05	0.04	9.96	bdl	5.15	2.81
K3-r	29.2	2.16	34.8	5.07	44.1	591	462	60	5.48	0.78	0.14	4.13	0.2	0.61	291	11.7	4.28	4.82	0.18	0.3	17.7	0.18	11.6	5.98
K3-f	38.8	2.22	7.18	3.07	59.5	621	594	96.9	3.92	0.92	0.16	4.63	0.22	0.52	412	14.6	6.72	3.1	0.08	0.16	15	0.07	14.2	3.29
K4-r	30.6	1.78	0.92	3.28	23.9	550	469	88.6	bdl	0.82	0.12	5.09	bdl	bdl	284	11.6	4.24	0.58	0.01	0.03	12.1	0.02	6.5	2.69
K4-p1	31.2	2.3	31.8	5.88	47.8	568	530	75.1	3.27	0.86	0.16	5.29	0.23	0.6	293	13.7	5.07	2.58	0.15	0.18	17.6	0.23	14.8	6.52
K4-f	40.3	2.48	7.78	2.95	5.73	180	696	100	1.83	1.13	0.2	6.52	0.15	bdl	52.5	17.7	8.1	3.07	0.14	0.05	15.8	0.19	2.95	6
K5-r	40	2.35	20.6	7.09	27.7	586	1154	184	11.4	1.92	0.25	11.6	0.45	bdl	146	33	14.5	3.28	0.21	0.4	28.6	0.32	34.6	12.2
K5-f	32.9	2.04	7.21	3.51	17.5	491	498	72.1	3.43	0.87	0.16	4.67	0.02	bdl	141	12.8	4.88	3.92	0.1	0.09	15.3	0.1	10.1	4.13
K7-r	31.3	2.37	2.65	3.32	3.62	578	772	115	1.08	2.99	0.18	6.55	bdl	bdl	179	19	7.92	2.16	0.06	0.03	7.51	0.15	11.1	3.81
K7-f	37.4	2.38	1.05	2.34	4.54	398	547	12.4	bdl	0.99	0.16	1.35	bdl	bdl	107	14	0.66	bdl	0.04	bdl	14.5	0.12	6.56	3.41
K8-r	28.6	2.41	1.54	2.05	7.98	401	257	11	bdl	0.49	0.1	1.25	bdl	bdl	151	6.72	0.58	bdl	0.05	0.01	7.21	bdl	2.13	1.41
K8-f	33	2.1	8.95	4.75	25.4	511	780	145	3.71	1.29	0.18	6.86	0.07	2.26	165	19.6	5.81	2.57	0.22	0.12	22.8	0.12	12.4	5.27
K10-r	27.3	1.55	4.09	1.48	17.6	485	286	37.3	0.36	0.5	0.09	2.44	bdl	bdl	136	6.94	2.45	4.11	0.1	0.04	10.7	0.02	6.81	1.69
K10-p1	26.1	2.42	5.26	1.81	18.3	422	318	40.6	0.3	0.56	0.1	2.66	bdl	bdl	120	7.49	2.55	3.15	0.19	0.15	7.23	0.01	6.62	1.63
K10-p2	25	1.36	5.19	1.97	15.9	350	267	36.8	1.31	0.6	0.08	2.36	bdl	bdl	139	6.64	2.28	6.04	0.25	0.08	17.8	0.01	5.73	1.25
K10-p3	31.6	2.19	28.9	5.56	8.74	511	597	99.1	3.66	0.94	0.17	5.29	0.16	bdl	1431	16	7.7	3.88	0.78	0.13	21.3	0.21	18.8	7.66
K10-p4	23	1.23	6.46	2.77	8.44	192	242	34.2	3.13	0.49	0.09	2.41	bdl	bdl	204	6.5	1.96	6.92	1.39	0.14	14.6	0.02	3.87	1.54
K10-p5	4.55	0.66	19.1	8.42	0.95	726	165.5	8.35	8.92	0.36	0.02	0.8	bdl	0.22	2468	2.23	0.42	4.9	2.69	0.51	39.1	0.01	1.63	1.14
K10-f	23.6	1.4	1.96	0.56	15.6	450	244	21.5	bdl	0.41	0.09	1.91	bdl	bdl	245	6.05	0.96	1.31	0.11	0.08	9.07	bdl	3.62	1.25
Tuff	30.6	1.76	7.04	3.02	15.5	374	593	84.2	1.68	2.69	0.35	6.56	3.17	14.1	72.1	14.74	9.91	6.74	0.96	0.37	30.9	0.89	16.7	12

av: average; bdl: below detection limit.

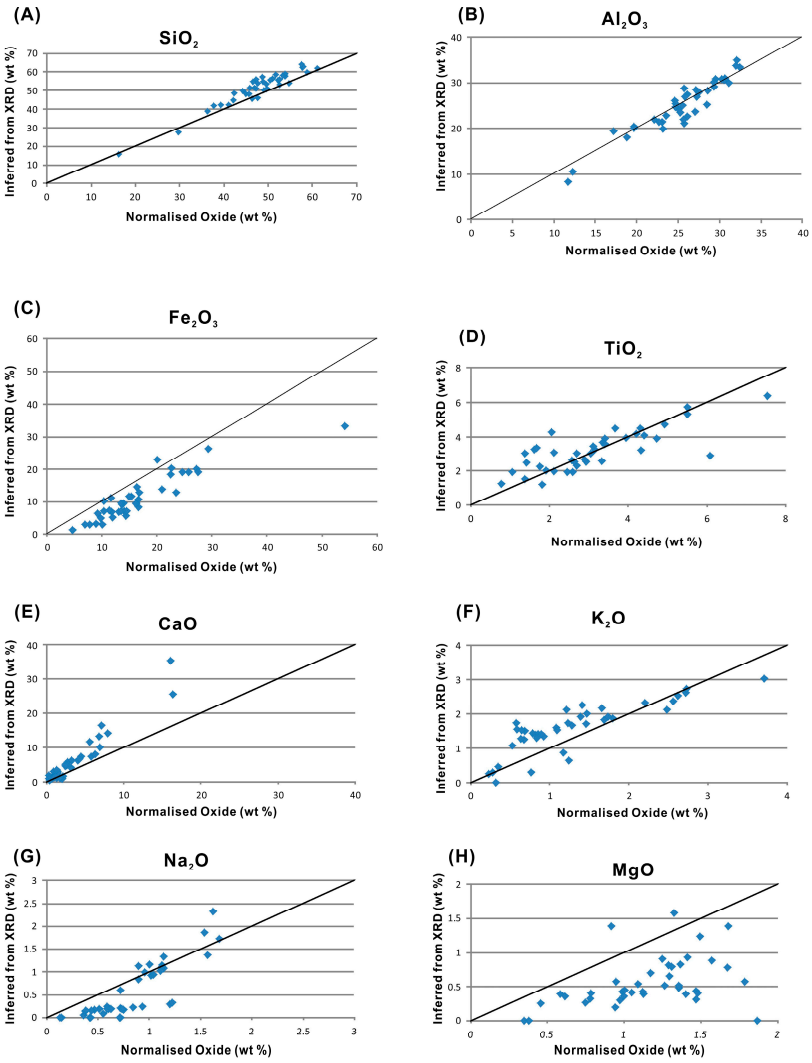

Figure 6. Comparison of observed oxide percentages from chemical analysis (*x*-axis) to oxide percentages inferred from XRD data (*y*-axis) in the Zhongliangshan coal and non-coal samples. The diagonal line in each plot indicates equality.

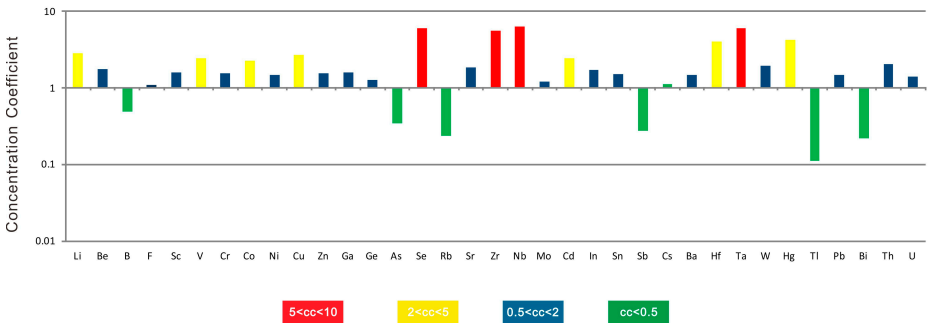

Figure 7. Concentration coefficients (CC) of trace elements in the Zhongliangshan coals, normalized by average trace element concentrations in the word hard coals [44].

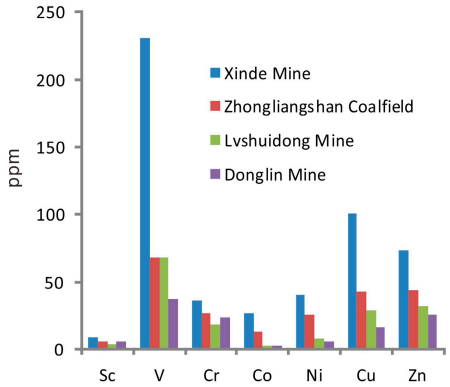

Figure 8. Concentration comparison of Sc, V, Cr, Co, Ni, Cu and Zn in the Xinde Mine, Zhongliangshan Coalfield, Lvshuidong Mine and Donglin Mine. The data of the Xinde, Lvshuidong and Donglin are from Dai et al. and Chen et al., respectively [8,14].

In order to describe the REY distribution in coals more conveniently, a three-fold geochemical classification and three enrichment types were proposed by Seredin and Dai [58]. Accordingly, normalized to the upper continental crust (UCC) [60], three enrichment types of REY in coal were generally identified: L-type (light-REY; La_N/Lu_N >1), M-type (medum-REY; La_N/Sm_N <1, Gd_N/Lu_N >1), and H-type (heavy-REY; La_N/Lu_N <1) [58]. In addition, several REY geochemical parameters (e.g., Ce_N/Ce_N*, Eu_N/Eu_N*, La_N/La_N*, Gd_N/Gd_N* and Y_N/Ho_N) are often used to rebuild the geochemical history [54,61], to recognize the sediment-source region [10,13,52,62], and to explain the tectonic evolution of coal deposits [3,63,64]. The REY concentrations and parameters of the Zhongliangshan coals are listed in Tables 4 and 5. The content of REY varies from 112 to 396 μg/g and averages 171 μg/g, higher than that in common world hard coals [47].

Table 4. Concentrations of rare earth element and yttrium (REY) in the coal and non-coal samples from the ZK4-1 drill core in the Zhongliangshan Coalfield (μg/g).

Sample	La	Ce	Pr	Nd	Sm	Eu	Gd	Tb	Dy	Y	Ho	Er	Tm	Yb	Lu
K1-1	30.19	61.66	6.74	25.12	4.61	0.80	4.69	0.68	4.10	20.75	0.78	2.29	0.31	2.08	0.28
K1-2	26.41	55.90	6.26	23.70	4.35	0.72	4.26	0.61	3.70	18.29	0.71	2.13	0.30	2.04	0.29
K1-av.	28.30	58.78	6.50	24.41	4.48	0.76	4.47	0.65	3.90	19.52	0.75	2.21	0.30	2.06	0.29
K2	24.91	46.70	5.03	18.31	3.33	0.49	3.47	0.49	3.10	16.86	0.62	1.88	0.26	1.74	0.24
K3	31.14	67.30	7.58	29.40	5.82	1.17	5.86	0.79	4.47	21.88	0.85	2.50	0.34	2.35	0.33
K4-1	18.59	40.32	4.64	18.38	3.53	0.66	3.54	0.48	2.84	14.89	0.54	1.61	0.22	1.49	0.21
K4-2	33.14	68.48	7.67	30.22	5.91	1.07	5.78	0.78	4.44	20.95	0.78	2.26	0.29	1.96	0.26
K4-av.	25.87	54.40	6.15	24.30	4.72	0.87	4.66	0.63	3.64	17.92	0.66	1.94	0.26	1.73	0.23
K5	19.00	40.48	4.78	18.68	3.86	0.83	4.38	0.68	4.34	27.84	0.91	2.93	0.42	2.99	0.45
K7	63.94	156.86	17.58	71.19	12.72	1.63	11.06	1.36	7.57	40.43	1.45	4.52	0.63	4.34	0.62
K8	29.99	66.55	7.68	29.70	5.92	1.01	6.08	0.85	5.10	26.63	0.99	2.99	0.42	2.82	0.40
K10-1	21.08	46.23	5.28	20.39	3.87	0.63	3.98	0.55	3.36	16.50	0.63	1.96	0.27	1.88	0.25
K10-2	24.71	50.94	5.75	22.09	4.26	0.71	4.41	0.64	3.91	20.05	0.74	2.20	0.29	2.00	0.27
K10-3	28.30	56.05	6.21	23.79	4.87	0.80	5.25	0.82	4.97	25.35	0.93	2.71	0.37	2.46	0.35
K10-4	31.58	58.60	6.54	24.75	4.17	0.76	4.27	0.56	3.22	17.54	0.62	1.87	0.26	1.81	0.25
K10-5	32.11	60.13	6.67	25.44	4.28	0.70	4.35	0.57	3.48	19.18	0.67	2.12	0.29	2.01	0.28
K10-av.	27.56	54.39	6.09	23.29	4.29	0.72	4.45	0.63	3.79	19.73	0.72	2.17	0.30	2.03	0.28
Average	29.65	62.59	7.03	27.23	5.11	0.86	5.10	0.70	4.18	21.94	0.80	2.43	0.33	2.28	0.32
K1-r	52.89	124.00	14.15	60.55	14.23	3.39	14.83	1.98	10.34	43.43	1.81	4.86	0.61	4.02	0.56
K1-p1	55.04	70.46	13.94	54.39	10.34	2.64	10.83	1.47	8.09	32.61	1.41	3.87	0.51	3.55	0.47
K1-p2	46.54	107.26	12.98	57.37	14.57	3.98	14.62	1.79	9.27	44.43	1.64	4.57	0.59	3.96	0.55
K1-p3	44.44	99.74	11.49	46.97	9.52	2.40	9.37	1.31	7.25	30.67	1.28	3.54	0.46	3.07	0.41
K1-f	55.60	124.12	14.31	58.63	11.40	2.88	11.16	1.51	8.49	37.37	1.51	4.34	0.57	3.73	0.51
K2-r	43.27	101.87	11.78	48.84	10.07	2.62	9.61	1.25	6.95	31.50	1.26	3.68	0.47	3.15	0.42
K2-f	39.72	98.05	11.73	51.46	11.16	3.26	11.10	1.42	7.49	25.60	1.31	3.66	0.47	3.14	0.43
K3-r	66.65	153.79	16.73	65.34	11.30	2.75	11.24	1.48	8.78	37.87	1.69	5.04	0.69	4.63	0.63
K3-f	80.74	170.00	20.50	82.13	15.14	3.65	13.75	1.74	9.56	38.05	1.68	4.64	0.60	4.03	0.55
K4-r	50.78	122.00	13.59	56.28	10.81	2.83	10.77	1.45	8.10	25.14	1.46	4.11	0.54	3.56	0.48
K4-p1	76.76	146.10	18.32	70.21	10.97	2.10	11.33	1.73	11.01	54.95	2.18	6.65	0.92	6.25	0.88
K4-f	19.89	91.23	5.98	23.29	4.17	0.95	4.45	0.68	3.99	9.99	0.82	2.39	0.38	2.31	0.34
K5-r	157.76	344.58	43.36	176.25	37.43	5.95	38.26	5.22	29.52	144.61	5.54	16.45	2.24	15.20	2.10

Table 4. *Cont.*

Sample	La	Ce	Pr	Nd	Sm	Eu	Gd	Tb	Dy	Y	Ho	Er	Tm	Yb	Lu
K5-f	56.64	130.14	15.03	62.04	12.23	2.49	12.58	1.84	10.39	48.68	1.96	5.55	0.76	5.22	0.71
K7-r	74.06	178.61	19.23	73.51	12.87	1.61	13.20	1.99	12.58	39.27	2.52	7.77	1.09	7.39	1.03
K7-f	48.00	125.68	13.88	55.87	10.12	1.86	9.81	1.46	8.74	21.61	1.64	4.91	0.64	4.35	0.59
K8-r	17.88	46.57	5.22	22.04	5.08	1.58	5.29	0.74	4.14	8.15	0.71	2.01	0.26	1.76	0.23
K8-f	82.29	186.95	21.47	84.09	16.00	2.58	15.86	2.35	14.15	42.00	2.73	8.27	1.15	7.91	1.10
K10-r	24.82	48.92	6.91	29.29	6.80	2.26	7.36	1.12	6.67	29.05	1.22	3.58	0.48	3.35	0.45
K10-p1	35.35	76.02	10.33	44.95	9.91	2.74	10.20	1.45	7.83	33.64	1.39	3.91	0.52	3.58	0.49
K10-p2	23.63	55.06	7.43	33.06	7.83	2.33	8.03	1.06	5.85	25.88	1.01	2.83	0.36	2.46	0.34
K10-p3	76.32	152.23	16.90	63.18	11.38	2.26	12.34	1.84	10.99	47.24	2.06	6.00	0.81	5.39	0.76
K10-p4	20.25	33.54	5.51	21.88	4.18	0.88	3.98	0.60	3.62	11.80	0.66	1.93	0.26	1.83	0.23
K10-p5	4.61	9.51	1.34	6.04	1.86	0.94	2.40	0.42	2.92	13.28	0.57	1.72	0.24	1.78	0.23
K10-f	16.20	33.11	4.14	16.47	3.47	0.97	3.61	0.55	3.40	10.07	0.63	1.93	0.27	1.88	0.25
Tuff	33.74	127.59	11.73	52.97	12.68	2.77	10.92	1.68	9.75	42.22	1.92	5.71	0.84	5.27	0.78

Table 5. REY parameters in the coal and non-coal samples from the ZK4-1 drill core in the Zhongliangshan Coalfield.

Sample	REY (μg/g)	La_N/Lu_N	La_N/Sm_N	Gd_N/Lu_N	Enrichment Type	Ce_N/Ce_N^*	Eu_N/Eu_N^*	Y_N/Ho_N	Gd_N/Gd_N^*	La_N/La_N^*
K1-1	165.06	1.07	0.98	1.31	L and M	0.99	0.79	0.97	1.13	1.10
K1-2	149.67	0.92	0.91	1.17	M and H	0.99	0.77	0.93	1.12	1.07
K2	127.44	1.05	1.12	1.15	L	0.95	0.67	0.99	1.15	1.16
K3	181.77	0.94	0.80	1.40	M and H	1.00	0.92	0.94	1.18	1.10
K4-1	111.96	0.90	0.79	1.36	M and H	0.99	0.86	1.01	1.17	1.14
K4-2	183.99	1.28	0.84	1.76	L and M	0.98	0.84	0.97	1.17	1.21
K5	132.56	0.43	0.74	0.77	H	0.97	0.93	1.11	1.10	1.09
K7	395.90	1.03	0.75	1.40	L and M	1.07	0.63	1.01	1.19	1.09
K8	187.13	0.75	0.76	1.20	M and H	1.00	0.77	0.98	1.15	1.04
K10-1	126.86	0.83	0.82	1.24	M and H	1.00	0.74	0.95	1.17	1.06
K10-2	142.97	0.91	0.87	1.28	M and H	0.97	0.75	0.99	1.13	1.13
K10-3	163.23	0.82	0.87	1.20	M and H	0.96	0.73	0.99	1.09	1.19
K10-4	156.80	1.28	1.14	1.36	L	0.93	0.83	1.03	1.21	1.23
K10-5	162.28	1.15	1.13	1.23	L	0.94	0.75	1.04	1.20	1.25
K1-r	351.67	0.94	0.56	2.09	M and H	1.03	1.07	0.87	1.20	1.34
K1-p1	269.61	1.18	0.80	1.83	L and M	0.58	1.14	0.84	1.19	1.07
K1-p2	324.12	0.84	0.48	2.08	M and H	1.00	1.25	0.99	1.25	1.45
K1-p3	271.92	1.09	0.70	1.81	L and M	1.01	1.17	0.87	1.14	1.19
K1-f	336.11	1.09	0.73	1.73	L and M	1.00	1.17	0.90	1.16	1.21
K2-r	276.75	1.02	0.64	1.79	L and M	1.03	1.22	0.91	1.19	1.18
K2-f	270.00	0.92	0.53	2.03	M and H	1.04	1.35	0.71	1.22	1.33
K3-r	388.60	1.06	0.88	1.41	L and M	1.05	1.12	0.82	1.19	1.09
K3-f	446.74	1.48	0.80	1.98	L and M	0.95	1.16	0.83	1.19	1.15
K4-r	311.90	1.05	0.70	1.75	L and M	1.06	1.20	0.63	1.17	1.20
K4-p1	420.36	0.88	1.05	1.02	H	0.89	0.87	0.92	1.09	1.09
K4-f	170.86	0.59	0.72	1.04	M and H	1.91	1.01	0.44	1.10	0.90
K5-r	1024.47	0.75	0.63	1.44	M and H	0.95	0.72	0.95	1.17	1.10
K5-f	366.26	0.79	0.69	1.39	M and H	1.02	0.92	0.90	1.12	1.20
K7-r	446.73	0.72	0.86	1.01	M and H	1.08	0.57	0.57	1.10	1.00
K7-f	309.15	0.81	0.71	1.31	M and H	1.11	0.86	0.48	1.09	1.02
K8-r	121.64	0.77	0.53	1.81	M and H	1.10	1.40	0.42	1.16	1.16
K8-f	488.91	0.75	0.77	1.14	M and H	1.01	0.74	0.56	1.10	1.05
K10-r	172.28	0.55	0.55	1.28	M and H	0.85	1.47	0.86	1.11	1.24
K10-p1	242.30	0.73	0.54	1.66	M and H	0.91	1.25	0.88	1.15	1.30
K10-p2	177.16	0.70	0.45	1.89	M and H	0.95	1.35	0.93	1.20	1.32
K10-p3	409.70	1.01	1.01	1.28	L	0.97	0.88	0.83	1.13	1.12
K10-p4	111.15	0.86	0.73	1.34	M and H	0.72	0.99	0.65	1.07	1.05
K10-p5	47.87	0.20	0.37	0.81	H	0.87	2.04	0.85	1.04	1.50
K10-f	96.95	0.65	0.70	1.14	M and H	0.92	1.26	0.58	1.09	1.12
Tuff	320.57	0.43	0.40	1.11	M and H	1.46	1.08	0.80	1.03	1.27

Note: REY, sum of La, Ce, Pr, Nd, Sm, Eu, Gd, Tb, Dy, Y, Ho, Er, Tm, Yb, and Lu; La_N/Lu_N, ratio of La_N and Lu_N; La_N/Sm_N, ratio of La_N and Sm_N; Gd_N/Lu_N, ratio of Gd_N and Lu_N; Y_N/Ho_N, ratio of Y_N and Ho_N; $Ce_N/Ce_N^* = Ce_N/(0.5La_N + 0.5Pr_N)$; $Eu_N/Eu_N^* = Eu_N/(0.5Sm_N + 0.5Gd_N)$; $Gd_N/Gd_N^* = Gd_N/[(Sm_N \times 0.33) + (Tb_N \times 0.67)$; $La_N/La_N^* = La_N/(3Pr_N\text{-}2Nd_N)$; N, REY are normalized by Upper Continental Crust (UCC) [60].

The Zhongliangshan coals, characterized by negative Ce, Eu anomalies and positive Gd, La anomalies, with no pronounced Y anomalies (Figure 9), are dominated by M-H type and, to a lesser extent, L- and L-M types, along with H-type (Table 5). The REY has a weakly positive correlation with ash yield in the Zhongliangshan coals (Figure 10A). This indicates that the modes of occurrences of REY may be not only associated with the mineral matter, but also with the organic matter in the coal. Some studies have shown that the correlation coefficients of REY with ash yields decrease along with atomic numbers [10,52,62,65]. However, the correlation coefficients between REY and ash yields in present study increase from 0.28 ($r_{La\text{-}Ash}$) to 0.79 ($r_{Lu\text{-}Ash}$) (Figure 10B) with the increasing atomic

number, similar to the trend of Haerwusu coals [66]. This probably suggests that the light REY have a mixed inorganic-organic affinity and the heavy REY have an inorganic-dominated affinity. It can be inferred that the ability being absorbed on the organic matter of LREY is higher than that of HREY, leading to higher HREY-ash correlation coefficients than those of LREY-ash pair [66].

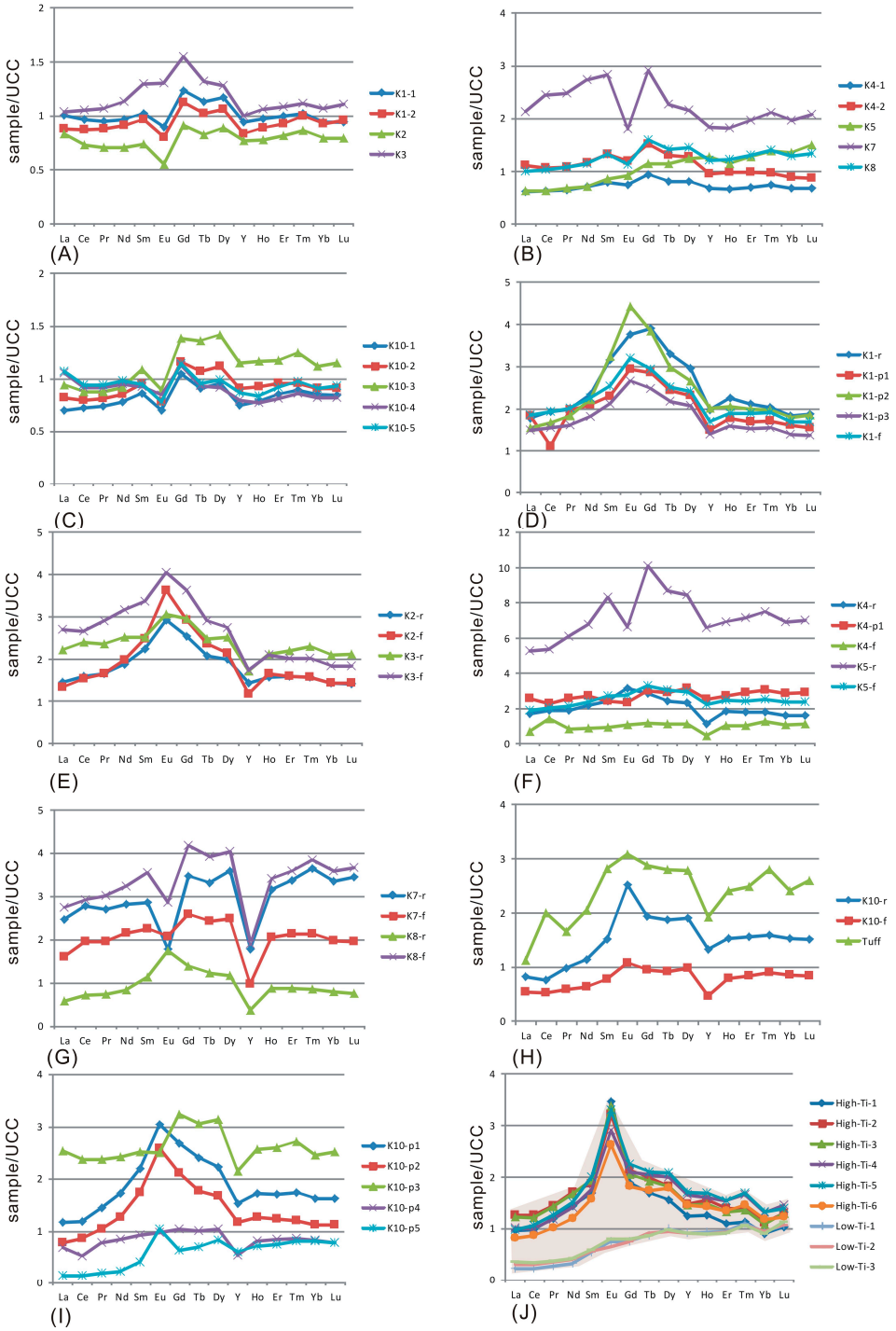

Figure 9. Upper Continental Crust-normalized REY patterns of samples from the Zhongliangshan coals (**A**–**C**); non-coal bands (**D**–**I**); and Emeishan high-Ti and low-Ti basalts (**J**). Note: the data of high-Ti and low-Ti are from Huang et al. [67].

4.4. Sediment Source Region

It is suggested that the dominant terrigenous material of the Lopingian coals in southwestern China is the basaltic Kangdian Upland, which is typically enriched in Sc, V, Cr, Co, Ni, Cu and Zn [10,45,64,68–71]. For example, the dominant terrigenous material for the coals in the Xinde Mine, Yunnan Province, southwestern China is identified as the Kangdian Upland, with high concentrations of Sc, V, Cr, Co, Ni, Cu and Zn in the coals [45]. The dominant terrigenous material of the Huayingshan and Nantong coalfields has also been considered to be the Kangdian Upland [11,12]. However, some studies have shown that, instead of the Kangdian Upland, the dominant terrigenous materials of Huayingshan and Nantong coalfields are the Leshan-Longnvsi Uplift, Hannan Upland, and Dabashan Uplift [8,13]. The abundances of Sc, V, Cr, Co, Ni, Cu and Zn in the Huayingshan Coalfield are only 3.54 μg/g, 68.4 μg/g, 18.8 μg/g, 3.03 μg/g, 7.96 μg/g, 29.2 μg/g and 31.5 μg/g, respectively [8], while those in the Nantong coalfield are 5.81 μg/g, 37.3 μg/g, 23.4 μg/g, 2.87 μg/g, 6.32 μg/g, 16.3 μg/g and 26 μg/g, respectively [13]. A number of studies have indicated that the coals with sediment source region consisted of felsic rocks have high concentration of lithophile elements but are low in V, Cr, Co, Ni, Cu and Zn [72–74].

In present study, the concentrations of Sc, V, Cr, Co, Ni, Cu and Zn are not as high as those in the Xinde Mine, and not as low as those in the Huayingshan and Nantong coalfields, neither (Figure 8). This may indicate that the Kangdian Upland is not the dominant sediment source region for the Zhongliangshan coals.

Many studies have shown that the Al_2O_3/TiO_2 ratios are useful provenance indicators to determine the terrigenous materials not only for normal sedimentary rocks but also for coal seams [8,10,73,75,76]. It is suggested that the Al_2O_3/TiO_2 ratios for sedimentary rocks with 3–8, 8–21, and 21–70 are considered to originate from mafic-, intermediate-, and felsic dominated sediment source regions, respectively [75]. In the plot of Al_2O_3 vs. TiO_2 for coal samples from the Zhongliangshan coalfield (Figure 11), almost all coal samples fall in the area between 8 and 21, indicating that the terrigenous source of the studied samples is of intermediate composition. This further indicates that the dominant sediment source region is not the mafic basalts of the Kangdian upland, where the typical Al_2O_3/TiO_2 ratios are between 3 and 8 [76].

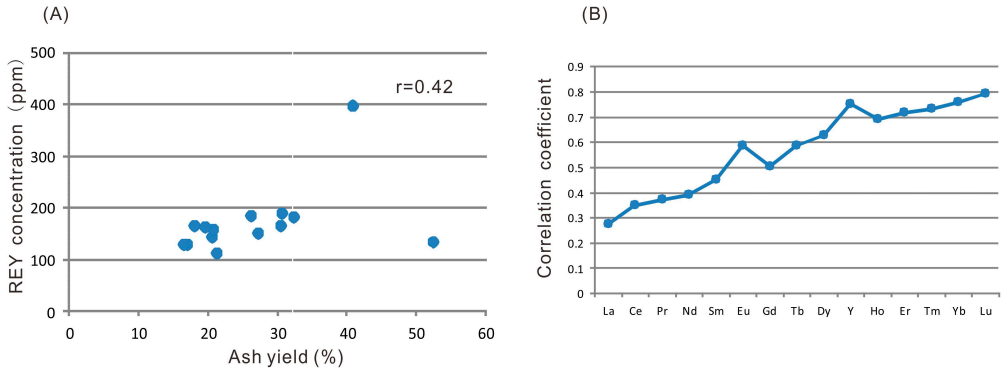

Figure 10. Relations between REY and ash yield (**A**); and between REY-ash correlation coefficients and REY atomic number (**B**).

Eu anomalies in coal can also be used as an indicator to interpret the sediment source region [51]. This is because Eu anomalies in coal are usually inherited from rocks within the sediment source region, and would not be affected between the weathering and transportation processes from the sediment source region to the peat swamp [51,52,77,78]. However, Eu anomalies may be influenced under the conditions of high-temperature hydrothermal fluids (>200 °C) and extremely reducing conditions [79,80].

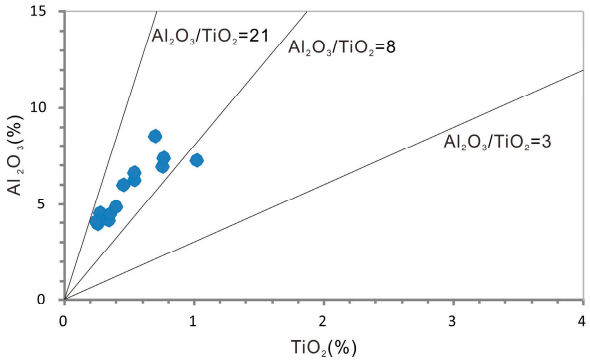

Figure 11. Al_2O_3 vs. TiO_2 for coal samples from the Zhongliangshan Coalfield.

Generally, coals with input of felsic or felsic-intermediate terrigenous materials usually have pronounced negative Eu anomalies [51], with a few exceptions of coals characterized by positive Eu anomalies that are caused by high content of plagioclase and other feldspars [81]. On the contrary, coals with input of mafic basalts display strongly positive Eu anomalies [45]. Chen et al. consider that the dominant terrigenous material of the Lopingian coals in the Nantong Coalfield is not the Kangdian Upland using the Eu anomalies. Dai et al. used the Eu anomalies to identify that the Yishan coals have been influenced by high-temperature hydrothermal solutions [10]. However, not all the coals influenced by hydrothermal solutions should have positive Eu anomalies [82]. For example, in some cases, coals or stone coals affected by hydrothermal solutions have a weak negative anomaly because the felsic sediment input overlapped the hydrothermal solutions [82].

The Figure 9 shows that almost all coals present distinctive negative Eu anomalies, different from the Emeishan basalts. This further indicates that the dominant terrigenous material is not the basalt of Kangdian Upland.

Note that there are some other three uplands/uplifts (TUUs) including the Leshan-Longnvsi uplift, Hannan Upland, and Dabashan Uplift around the Zhongliangshan coalfield (Figure 1). Dai et al. have proposed that TUUs are the dominant terrigenous materials for the Huayingshan coalfield [8]. Hence, the dominant sediment source region of present study may also be TUUs. However, based on the abundances of Sc, V, Cr, Co, Ni, Cu and Zn in the Zhongliangshan coals and the proximity to the Kangdian Upland, the Kangdian Upland may also provide a small proportion of terrigenous materials for the Zhongliangshan Coalfield.

4.5. Injection of Low-Temperature Hydrothermal Fluids

Hydrothermal fluid activity plays an important role in the enrichment of mineral matter in the coals not only from southwestern China [2,40,43,83–88], but also from some coal deposits elsewhere [89–91]. However, the characteristics and alteration mechanism of hydrothermal solution are not clear. Recently, Dai et al. illustrate the hydrothermal solution compositions, nature and mineralization of the alkali volcanic ash in Yunnan Province (southwestern China) based on the analysis of H-O isotope and petrological, mineralogical and geochemical assemblages [92]. Firstly, the alkali volcanic ash was leached by the mixed high-temperature hydrothermal solution (including acidic waters and CO_2 degassing from the Emeishan Plume) and resulted in the in situ enrichment of Al, Ti and the depletion of Nb, Zr, Ga and REY [92]. Secondly, the leached Nb, Zr, Ga and REY were precipitated under the environment of cooler, neutral or alkaline hydrothermal fluid alteration [92], and in some cases, with injection of sea water [93].

Chamosite is not usually observed in the coal, however, it does commonly occur in the Lopingian coals in southwestern China [39,40,42,45,49]. Two origins of chamosite have been proposed, which is either derived from the alteration of kaolinite by the injection of Fe-Mg-rich fluids during diagenesis process [40], or directly precipitated from hydrothermal fluids enriched Fe [49].

The coexistence of chamosite and kaolinite and their close relationship (Figure 3C,D) indicate that chamosite was the interaction product between the kaolinite and Fe-Mg-rich fluids, which is similar to the mechanism reported by Dai and Chou [40]. Chamosite of hydrothermal origin was also observed (Figure 3E), where chamosite was independent of kaolinite and occurred as cell-fillings.

Besides chamosite, the modes of occurrence of barite (Figure 5F) and rhabdophane (Figure 5G) in the coal also illustrate that these minerals were precipitated from hydrothermal fluids. Barite has been indicated to be formed by the injection of hydrothermal fluids [8]. Rhabdophane is often observed in some REY-rich coals and derived from hydrothermal fluids in southwestern China [8,39,45,84].

The cell-filling quartz (Figure 4D,E) indicates an authigenic origin. In addition, calcite in the present study, which infills cell (Figure 4G,H) and fracture cavities (Figure 5A) indicate an epigenetic origin.

Based on the strong negative Eu anomalies of coals (Figure 9), the temperature of hydrothermal fluids may be all relatively low (<200 °C), although the multi-stage injection of hydrothermal fluids has been put forward. Otherwise, the Eu anomaly would be expected to be strong positive due to the ingress of hydrothermal fluids at >200 °C during the peatification, in that the reduction of Eu requires not only extremely reducing conditions but also high-temperature [10,51].

4.6. Evaluation of Rare Metals

Some Lopingian coals or non-coal strata in southwestern China are considered as potential economic sources for critical metals including Nb, Zr, Ga and REY [7,8,14,94]. In order to assess the REY in coal ashes as economic raw materials, several criteria (including the REY cut-off grade and the individual elemental composition) were proposed by Seredin and Dai [58]. Seredin and Dai have also proposed the cut-off grade for recovery from the coal ash (REY oxides (REO) $\geq$ 1000 μg/g) [58]. Based on the classification reported by Dai et al. [9], the C_{outl}-REO graph is plotted in Figure 12 to evaluate industrial potential of REY in present study (C_{outl} = [(Nd + Eu + Tb + Dy + Er + Y)/ΣREY]/[(Ce + Ho + Tm + Yb + Lu)/ΣREY]) [58]. It can be obtained that the REY concentrations in most samples of the Zhongliangshan coals are lower than the cut-off grade except for samples K1-1, K7 and K5-r. Thus, the K7 and the upper portion of K1 have the potential to be a source of raw material for REY recovery. However, the K2, K3, K4, K5, K8 and K10 coals cannot be considered as REY raw material sources. It is noted that some coal seams in other coalfields surrounding Zhongliangshan coalfield enrich REY (Figure 13), where the REO in coal ash are higher than 1000 ppm. However, the REY data in the Shuijiang, Nantong, Xishui, Junlian, and Furong Coalfields, are lower than the cut-off grade or absent, which needs further research.

In addition to factors as mentioned above that could lead to enrichment of REY in coal deposit, some other factors such as alkaline volcanic ashes [95] and to a lesser extent, ground water leaching [96], can also play an important roles in the Lopingian coals. Similar to the K7 and the upper portion of K1 coal seams, the coals subjected to alkaline volcanic ashes and in some cases, groundwater leaching, usually have a high potential of REY [95,96].

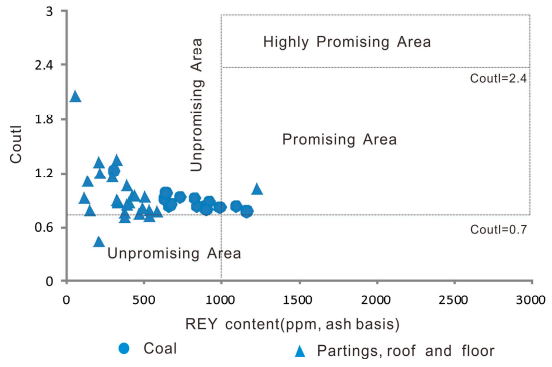

Figure 12. Evaluation of REY in the coal ashes and host rocks in the Zhongliangshan Coalfield. The classification base map is based on Dai et al. [9].

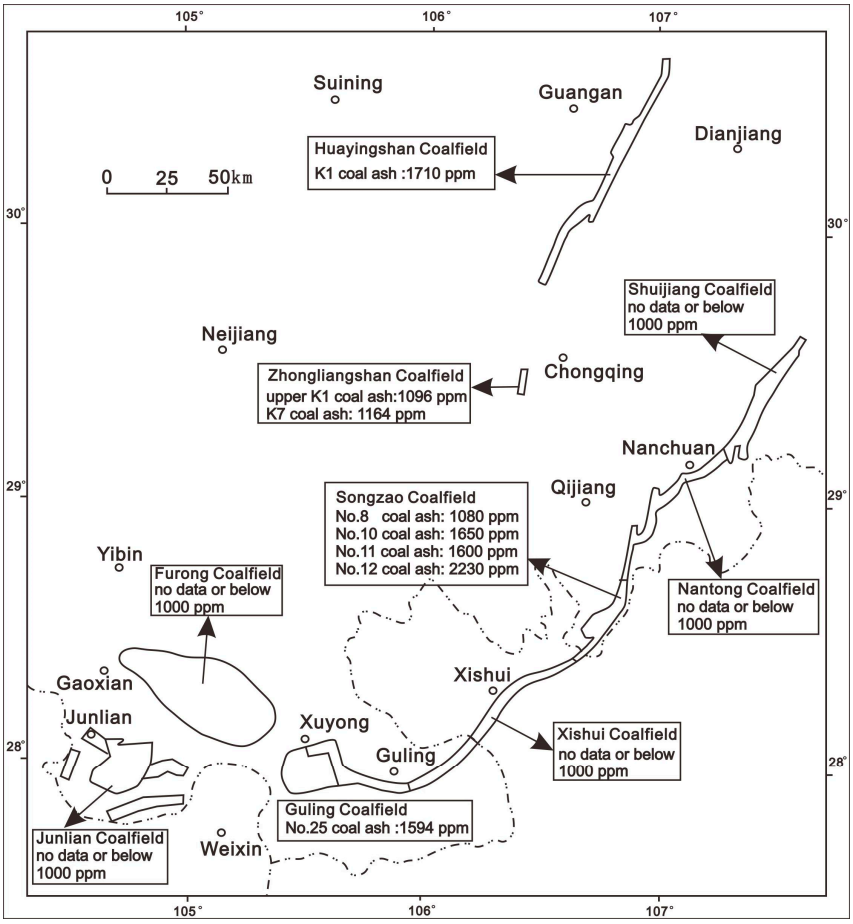

Figure 13. REY oxides (REO) concentrations in coal ash higher than 1000 ppm in Zhongliangshan and surrounding Coalfields. Tha data of Huayingshan Coalfield is from Dai et al. [8]. The data of the Songzao Coalfield is from Seredin and Dai [58]. The data of the Guxu Coalfield is from Dai et al. [82].

5. Conclusions

The Lopingian coals from the ZK4-1 drill core in the Zhongliangshan Coalfield are medium volatile bituminous coal, which are characterized by a medium-ash yield (26.84%) and high sulfur content (3.38%). Minerals in the Zhongliangshan coals are mainly composed of kaolinite, pyrite, quartz and calcite, with small proportions of anatase. The illite/smectite mixed layer (I/S), chamosite, rutile, marcasite, ankerite, dolomite, jarosite, natrojarosite, bassanite, gypsum and K-feldspar are also present in various coal samples. In addition, apatite, rhabdophane and barite are observed under the SEM-EDX although they are below the detection limit of the XRD.

Compared with the average concentrations of the world hard coals [47], some trace elements including Li, V, Co, Cu, Se, Y, Zr, Nb, REE, Cd, Ta, Hf and Hg, are enriched in the Zhongliangshan coals. Based on the concentrations of Sc, V, Cr, Co, Ni, Cu and Zn, the ratios of Al_2O_3/TiO_2 and the UCC-normalized REY distribution patterns of the Zhongliangshan coals, the dominant sediment source region are the Leshan-Longnvsi Uplift, Hannan Upland, and Dabashan, Uplift, with a small proportion of terrigenous materials from the Kangdian Upland. The modes of occurrence of chamosite, barite, rhabdophane, quartz and calcite indicate that the Zhongliangshan coals have probably been affected by the injection of different low-temperature hydrothermal fluids. The K7 and the upper portion of K1 have the potential to be a source of raw material for REY recovery.

Acknowledgments: This research was funded by the National Key Basic Research and Development Program (No. 2014CB238902), National Natural Science Foundation of China (No. 41502162), the "111" Project (No. B17042)

and Chongqing Performance Incentive Project (No. cstc2017jxjl90013). We are indebted to Zhen Wang for his assistance of geochemical analysis. We thank Lei Zhao for the suggestions during the manuscript preparing and revising. Thanks are given to the editor and two anonymous reviewers for their constructive suggestions.

Author Contributions: Jianhua Zou conducted the SEM-EDX data, interpreted all of the data and composed the manuscript. Feng Han, Tian Li, Heming Tian and Yingjiao Li collected the exploratory drill core samples (ZK4-1) and were responsible for the chemical and mineralogy analysis.

Conflicts of Interest: The authors declare no conflict of interest.

References

1. Dai, S.; Zeng, R.; Sun, Y. Enrichment of arsenic, antimony, mercury, and thallium in a Late Permian anthracite from Xingren, Guizhou, Southwest China. *Int. J. Coal Geol.* **2006**, *66*, 217–226. [CrossRef]
2. Dai, S.; Ren, D.; Chou, C.-L.; Finkelman, R.B.; Seredin, V.V.; Zhou, Y. Geochemistry of trace elements in Chinese coals: A review of abundances, genetic types, impacts on human health, and industrial utilization. *Int. J. Coal Geol.* **2012**, *94*, 3–21. [CrossRef]
3. Luo, K.; Ren, D.; Xu, L.; Dai, S.; Cao, D.; Feng, F.; Tan, J. Fluorine content and distribution pattern in Chinese coals. *Int. J. Coal Geol.* **2004**, *57*, 143–149. [CrossRef]
4. Tian, L.; Dai, S.; Wang, J.; Huang, Y.; Ho, S.C.; Zhou, Y.; Lucas, D.; Koshland, C.P. Nanoquartz in Late Permian C1 coal and the high incidence of female lung cancer in the Pearl River Origin area: A retrospective cohort study. *BMC Public Health* **2008**, *8*, 398. [CrossRef] [PubMed]
5. Zheng, B.; Ding, Z.; Huang, R.; Zhu, J.-M.; Yu, X.; Wang, A.; Zhou, D.; Mao, D.; Su, H. Issues of health and disease relating to coal use in southwestern China. *Int. J. Coal Geol.* **1999**, *40*, 119–132. [CrossRef]
6. Dai, S.; Finkelman, R.B. Coal as a promising source of critical elements: Progress and future prospects. *Int. J. Coal Geol.* **2018**, *186*, 155–164. [CrossRef]
7. Dai, S.; Zhou, Y.; Zhang, M.; Wang, X.; Wang, J.; Song, X.; Jiang, Y.; Luo, Y.; Song, Z.; Yang, Z.; et al. A new type of Nb (Ta)-Zr(Hf)-REE-Ga polymetallic deposit in the late Permian coal-bearing strata, eastern Yunnan, southwestern China: Possible economic significance and genetic implications. *Int. J. Coal Geol.* **2010**, *83*, 55–63. [CrossRef]
8. Dai, S.; Luo, Y.; Seredin, V.V.; Ward, C.R.; Hower, J.C.; Zhao, L.; Liu, S.; Zhao, C.; Tian, H.; Zou, J. Revisiting the late Permian coal from the Huayingshan, Sichuan, southwestern China: Enrichment and occurrence modes of minerals and trace elements. *Int. J. Coal Geol.* **2014**, *122*, 110–128. [CrossRef]
9. Dai, S.; Xie, P.; Jia, S.; Ward, C.R.; Hower, J.C.; Yan, X.; French, D. Enrichment of U-Re-V-Cr-Se and rare earth elements in the Late Permian coals of the Moxinpo Coalfield, Chongqing, China: Genetic implications from geochemical and mineralogical data. *Ore Geol. Rev.* **2017**, *80*, 1–17. [CrossRef]
10. Dai, S.; Xie, P.; Ward, C.R.; Yan, X.; Guo, W.; French, D.; Graham, I.T. Anomalies of rare metals in Lopingian super-high-organic-sulfur coals from the Yishan Coalfield, Guangxi, China. *Ore Geol. Rev.* **2017**, *88*, 235–250. [CrossRef]
11. Zhuang, X.; Su, S.; Xiao, M.; Li, J.; Alastuey, A.; Querol, X. Mineralogy and geochemistry of the Late Permian coals in the Huayingshan coal-bearing area, Sichuan Province, China. *Int. J. Coal Geol.* **2012**, *94*, 271–282. [CrossRef]
12. China National Administration of Coal Geology. *Sedimentary Environments and Coal Accumulation of Late Permian Coal Formation in Western Guizhou, Southern Sichuan and Eastern Yunnan, China*; Chongqing University Press: Chongqing, China, 1996.
13. Chen, J.; Chen, P.; Yao, D.; Liu, Z.; Wu, Y.; Liu, W.; Hu, Y. Mineralogy and geochemistry of Late Permian coals from the Donglin Coal Mine in the Nantong coalfield in Chongqing, southwestern China. *Int. J. Coal Geol.* **2015**, *149*, 24–40. [CrossRef]
14. Zou, J.; Tian, H.; Li, T. Geochemistry and Mineralogy of Tuff in Zhongliangshan Mine, Chongqing, Southwestern China. *Minerals* **2016**, *6*, 47. [CrossRef]
15. Zou, J.; Tian, H.; Wang, Z. Leaching Process of Rare Earth Elements, Gallium and Niobium in a Coal-Bearing Strata-Hosted Rare Metal Deposit—A Case Study from the Late Permian Tuff in the Zhongliangshan Mine, Chongqing. *Metals* **2017**, *7*, 174. [CrossRef]
16. Dai, S.; Ward, C.R.; Graham, I.T.; French, D.; Hower, J.C.; Zhao, L.; Wang, X. Altered volcanic ashes in coal and coal-bearing sequences: A review of their nature and significance. *Earth-Sci. Rev.* **2017**, *175*, 44–74. [CrossRef]

17. Zhao, L.; Dai, S.; Graham, I.T.; Li, X.; Zhang, B. New insights into the lowest Xuanwei Formation in eastern Yunnan Province, SW China: Implications for Emeishan large igneous province felsic tuff deposition and the cause of the end-Guadalupian mass extinction. *Lithos* **2016**, *264*, 375–391. [CrossRef]
18. Chen, X.; Xu, J.; Cheng, H.; Wang, M.; Chen, X.; Xu, A.; Deng, Z.; Wu, H.; Qiu, J.; Rong, J. Discussion on Hannan Upland and Dabashan Uplift. *J. Stratigr.* **1990**, *14*, 81–116, (In Chinese with an English abstract).
19. Jiang, Y.; Zhao, L.; Zhou, G.; Wang, X.; Zhao, L.; Wei, J.; Song, H. Petrological, mineralogical, and geochemical compositions of Early Jurassic coals in the Yining Coalfield, Xinjiang, China. *Int. J. Coal Geol.* **2015**, *152*, 47–67. [CrossRef]
20. ASTM International. *Test Method for Moisture in the Analysis Sample of Coal and Coke*; ASTM International: West Conshohocken, PA, USA, 2011.
21. ASTM International. *Test Method for Ash in the Analysis Sample of Coal and Coke*; ASTM International: West Conshohocken, PA, USA, 2011.
22. ASTM International. *Test Method for Volatile Matter in the Analysis Sample of Coal and Coke*; ASTM International: West Conshohocken, PA, USA, 2011.
23. ASTM International. *Standard Test for Total Sulfur in the Analysis Sample of Coal and Coke*; ASTM International: West Conshohocken, PA, USA, 2007.
24. ASTM International. *Standard Test Method for Forms of Sulfur in Coal*; ASTM International: West Conshohocken, PA, USA, 2012.
25. Rietveld, H.M. A profile refinement method for nuclear and magnetic structures. *Appl. Crystallogr.* **1969**, *2*, 65–71. [CrossRef]
26. Taylor, J.C. Computer Programs for Standardless Quantitative Analysis of Minerals Using the Full Powder Diffraction Profile. *Powder Diffr.* **1991**, *6*, 2–9. [CrossRef]
27. Ward, C.R.; Matulis, C.E.; Taylor, J.C.; Dale, L.S. Quantification of mineral matter in the Argonne Premium coals using interactive Rietveld-based X-ray diffraction. *Int. J. Coal Geol.* **2001**, *46*, 67–82. [CrossRef]
28. Ward, C.R.; Spears, D.A.; Booth, C.A.; Staton, I.; Gurba, L.W. Mineral matter and trace elements in coals of the Gunnedah Basin, New South Wales, Australia. *Int. J. Coal Geol.* **1999**, *40*, 281–308. [CrossRef]
29. Ruan, C.D.; Ward, C.R. Quantitative X-ray powder diffraction analysis of clay minerals in Australian coals using Rietveldmethods. *Appl. Clay Sci.* **2002**, *21*, 227–240. [CrossRef]
30. Li, X.; Dai, S.; Zhang, W.; Li, T.; Zheng, X.; Chen, W. Determination of As and Se in coal and coal combustion products using closed vessel microwave digestion and collision/reaction cell technology (CCT) of inductively coupled plasma mass spectrometry (ICP-MS). *Int. J. Coal Geol.* **2014**, *124*, 1–4. [CrossRef]
31. Dai, S.; Song, W.; Zhao, L.; Li, X.; Hower, J.C.; Ward, C.R.; Wang, P.; Li, T.; Zheng, X.; Seredin, V.V.; et al. Determination of Boron in Coal Using Closed-Vessel Microwave Digestion and Inductively Coupled Plasma Mass Spectrometry (ICP-MS). *Energy Fuels* **2014**, *28*, 4517–4522. [CrossRef]
32. Dai, S.; Seredin, V.V.; Ward, C.R.; Hower, J.C.; Xing, Y.; Zhang, W.; Song, W.; Wang, P. Enrichment of U–Se–Mo–Re–V in coals preserved within marine carbonate successions: Geochemical and mineralogical data from the Late Permian Guiding Coalfield, Guizhou, China. *Miner. Deposita* **2015**, *50*, 159–186. [CrossRef]
33. ASTM International. *Standard Test Method for Total Florine in Coal and Coke by pyrohydrolytic Extraction and Ion Selective Electrode or Ion Chromatograph Methods*; ASTM International: West Conshohocken, PA, USA, 2015.
34. ASTM International. *Standard Classification of Coals by Rank*; ASTM International: West Conshohocken, PA, USA, 2012.
35. Saikia, B.K.; Ward, C.R.; Oliveira, M.L.S.; Hower, J.C.; Baruah, B.P.; Braga, M.; Silva, L.F. Geochemistry and nano-mineralogy of two medium-sulfur northeast Indian coals. *Int. J. Coal Geol.* **2014**, *121*, 26–34. [CrossRef]
36. Saikia, B.K.; Ward, C.R.; Oliveira, M.L.S.; Hower, J.C.; De Leao, F.; Johnston, M.N.; O'Bryan, A.; Sharma, A.; Baruah, B.P.; Silva, L.F.O. Geochemistry and nano-mineralogy of feed coals, mine overburden, and coal-derived fly ashes from Assam (North-east India): A multi-faceted analytical approach. *Int. J. Coal Geol.* **2015**, *137*, 19–37. [CrossRef]
37. Saikia, B.K.; Saikia, A.; Choudhury, R.; Xie, P.; Liu, J.; Das, T.; Dekaboruah, H.P. Elemental geochemistry and mineralogy of coals and associated coal mine overburden from Makum coalfield (Northeast India). *Environ. Earth Sci.* **2016**, *75*, 660. [CrossRef]
38. Ward, C.R. Minerals in bituminous coals of the Sydney Basin (Australia) and the Illinois Basin (USA). *Int. J. Coal Geol.* **1989**, *13*, 455–479. [CrossRef]

39. Zhao, L.; Ward, C.R.; French, D.; Graham, I.T. Mineralogical composition of Late Permian coal seams in the Songzao Coalfield, southwestern China. *Int. J. Coal Geol.* **2013**, *116*, 208–226. [CrossRef]
40. Dai, S.; Chou, C.-L. Occurrence and origin of minerals in a chamosite-bearing coal of Late Permian age, Zhaotong, Yunnan, China. *Am. Mineral.* **2007**, *92*, 1253–1261. [CrossRef]
41. Moore, D.M.; Reynolds, R.C. *X-ray Diffraction and the Identification and Analysis of Clay Minerals*; Oxford University Press: New York, NY, USA, 1989.
42. Wang, P.; Yan, X.; Guo, W.; Zhang, S.; Wang, Z.; Xu, Y.; Wang, L. Geochemistry of Trace Elements in Coals from the Yueliangtian Mine, Western Guizhou, China: Abundances, Modes of Occurrence, and Potential Industrial Utilization. *Energy Fuels* **2016**, *30*, 10268–10281. [CrossRef]
43. Wang, X.; Dai, S.; Chou, C.-L.; Zhang, M.; Wang, J.; Song, X.; Wang, W.; Jiang, Y.; Zhou, Y.; Ren, D. Mineralogy and geochemistry of Late Permian coals from the Taoshuping Mine, Yunnan Province, China: Evidences for the sources of minerals. *Int. J. Coal Geol.* **2012**, *96*, 49–59. [CrossRef]
44. Xie, P.; Song, H.; Wei, J.; Li, Q. Mineralogical Characteristics of Late Permian Coals from the Yueliangtian Coal Mine, Guizhou, Southwestern China. *Minerals* **2016**, *6*, 29. [CrossRef]
45. Dai, S.; Li, T.; Seredin, V.V.; Ward, C.R.; Hower, J.C.; Zhou, Y.; Zhang, M.; Song, X.; Song, W.; Zhao, C. Origin of minerals and elements in the Late Permian coals, tonsteins, and host rocks of the Xinde Mine, Xuanwei, eastern Yunnan, China. *Int. J. Coal Geol.* **2014**, *121*, 53–78. [CrossRef]
46. Zhao, L.; Ward, C.R.; French, D.; Graham, I. Mineralogy of the volcanic-influenced Great Northern coal seam in the Sydney Basin, Australia. *Int. J. Coal Geol.* **2012**, *113*, 94–110. [CrossRef]
47. Ketris, M.P.; Yudovich, Y.E. Estimations of Clarkes for Carbonaceous biolithes: World averages for trace element contents in black shales and coals. *Int. J. Coal Geol.* **2009**, *78*, 135–148. [CrossRef]
48. Dai, S.; Tian, L.; Chou, C.-L.; Zhou, Y.; Zhang, M.; Zhao, L.; Wang, J.; Yang, Z.; Cao, H.; Ren, D. Mineralogical and compositional characteristics of Late Permian coals froman area of high lung cancer rate in Xuan Wei, Yunnan, China: Occurrence and origin of quartz and chamosite. *Int. J. Coal Geol.* **2008**, *76*, 318–327. [CrossRef]
49. Dai, S.; Ren, D.; Zhou, Y.; Chou, C.-L.; Wang, X.; Zhao, L.; Zhu, X. Mineralogy and geochemistry of a superhigh-organic-sulfur coal, Yanshan Coalfield, Yunnan, China: Evidence for a volcanic ash component and influence by submarine exhalation. *Chem. Geol.* **2008**, *255*, 182–194. [CrossRef]
50. Loges, A.; Wagner, T.; Barth, M.; Bau, M.; Göb, S.; Markl, G. Negative Ce anomalies in Mn oxides: The role of Ce4+ mobility during water–mineral interaction. *Geochim. Cosmochim. Acta* **2012**, *86*, 296–317. [CrossRef]
51. Dai, S.; Graham, I.T.; Ward, C.R. A review of anomalous rare earth elements and yttrium in coal. *Int. J. Coal Geol.* **2016**, *159*, 82–95. [CrossRef]
52. Eskenazy, G.M. Rare Earth Elements in a Sampled Coal from the Pirin Deposit, Bulgaria. *Int. J. Coal Geol.* **1987**, *7*, 301–314. [CrossRef]
53. Eskenazy, G.M. Aspects of the geochemistry of rare earth elements in coal an experimental approach. *Int. J. Coal Geol.* **1999**, *38*, 285–295. [CrossRef]
54. Hower, J.C.; Ruppert, L.F.; Eble, C.F. Lanthanide, yttrium, and zirconium anomalies in the Fire Clay coal bed, Eastern Kentucky. *Int. J. Coal Geol.* **1999**, *39*, 141–153. [CrossRef]
55. Hower, J.C.; Eble, C.F.; Dai, S.; Belkin, H.E. Distribution of rare earth elements in eastern Kentucky coals: Indicators of multiple modes of enrichment? *Int. J. Coal Geol.* **2016**, *160*, 73–81. [CrossRef]
56. Hower, J.; Granite, E.; Mayfield, D.; Lewis, A.; Finkelman, R. Notes on Contributions to the Science of Rare Earth Element Enrichment in Coal and Coal Combustion Byproducts. *Minerals* **2016**, *6*, 32. [CrossRef]
57. Seredin, V.V. Rare earth element-bearing coals from the Russian Far East deposits. *Int. J. Coal Geol.* **1996**, *30*, 101–129. [CrossRef]
58. Seredin, V.V.; Dai, S. Coal deposits as potential alternative sources for lanthanides and yttrium. *Int. J. Coal Geol.* **2012**, *94*, 67–93. [CrossRef]
59. Seredin, V.V.; Finkelman, R.B. Metalliferous coals: A review of the main genetic and geochemical types. *Int. J. Coal Geol.* **2008**, *76*, 253–289. [CrossRef]
60. Taylor, S.R.; Mclennan, S.H. *The Continental Crust: Its Composition and Evolution*; Blackwell: Oxford, UK, 1985.
61. Mardon, S.M.; Hower, J.C. Impact of coal properties on coal combustion by-product quality: Examples from a Kentucky power plant. *Int. J. Coal Geol.* **2004**, *59*, 153–169. [CrossRef]
62. Eskenazy, G.M. Rare earth elements and yttrium in lithotypes of Bulgarian coals. *Org. Geochem.* **1987**, *11*, 83–89. [CrossRef]

63. Dai, S.; Chekryzhov, I.Y.; Seredin, V.V.; Nechaev, V.P.; Graham, I.T.; Hower, J.C.; Ward, C.R.; Ren, D.; Wang, X. Metalliferous coal deposits in East Asia (Primorye of Russia and South China): A review of geodynamic controls and styles of mineralization. *Gondwana Res.* **2016**, *29*, 60–82. [CrossRef]
64. Zhao, L.; Dai, S.; Graham, I.T.; Li, X.; Liu, H.; Song, X.; Hower, J.C.; Zhou, Y. Cryptic sediment-hosted critical element mineralization from eastern Yunnan Province, southwestern China: Mineralogy, geochemistry, relationship to Emeishan alkaline magmatism and possible origin. *Ore Geol. Rev.* **2017**, *80*, 116–140. [CrossRef]
65. Querol, X.; Fernandez-Turiel, J.L.; Lopez-Soler, A. Trace elements in coal and their behaviour during combustion in a large power station. *Fuel* **1995**, *74*, 331–343. [CrossRef]
66. Dai, S.; Li, D.; Chou, C.-L.; Zhao, L.; Zhang, Y.; Ren, D.; Ma, Y.; Sun, Y. Mineralogy and geochemistry of boehmite-rich coals: New insights from the Haerwusu Surface Mine, Jungar Coalfield, Inner Mongolia, China. *Int. J. Coal Geol.* **2008**, *74*, 185–202. [CrossRef]
67. Huang, H.; Du, Y.; Yang, J.; Zhou, L.; Hu, L.; Huang, H.; Huang, Z. Origin of Permian basalts and clastic rocks in Napo, Southwest China: Implications for the erosion and eruption of the Emeishan large igneous province. *Lithos* **2014**, *208*, 324–338. [CrossRef]
68. Chen, J.; Algeo, T.J.; Zhao, L.; Chen, Z.; Cao, L.; Zhang, L.; Li, Y. Diagenetic uptake of rare earth elements by bioapatite, with an example from Lower Triassic conodonts of South China. *Earth Sci. Rev.* **2015**, *149*, 181–202. [CrossRef]
69. Liu, J.; Yang, Z.; Yan, X.; Ji, D.; Yang, Y.; Hu, L. Modes of occurrence of highly-elevated trace elements in superhigh-organic-sulfur coals. *Fuel* **2015**, *156*, 190–197. [CrossRef]
70. Luo, Y.; Zheng, M. Origin of Minerals and Elements in the Late Permian Coal Seams of the Shiping Mine, Sichuan, Southwestern China. *Minerals* **2016**, *6*, 74. [CrossRef]
71. Xie, P.; Zhang, S.; Wang, Z.; Wang, L.; Xu, Y. Geochemical characteristics of the Late Permian coals from the Yueliangtian Coalfield, western Guizhou, southwestern China. *Arab. J. Geosci.* **2017**, *10*, 98. [CrossRef]
72. Dai, S.; Ren, D.; Chou, C.-L.; Li, S.; Jiang, Y. Mineralogy and geochemistry of the No. 6 Coal (Pennsylvanian) in the Junger Coalfield, Ordos Basin, China. *Int. J. Coal Geol.* **2006**, *66*, 253–270. [CrossRef]
73. Dai, S.; Li, T.; Jiang, Y.; Ward, C.R.; Hower, J.C.; Sun, J.; Liu, J.; Song, H.; Wei, J.; Li, Q.; et al. Mineralogical and geochemical compositions of the Pennsylvanian coal in the Hailiushu Mine, Daqingshan Coalfield, Inner Mongolia, China: Implications of sediment-source region and acid hydrothermal solutions. *Int. J. Coal Geol.* **2015**, *137*, 92–110. [CrossRef]
74. Dai, S.; Hower, J.C.; Ward, C.R.; Guo, W.; Song, H.; O'Keefe, J.M.K.; Xie, P.; Hood, M.M.; Yan, X. Elements and phosphorusminerals in the middle Jurassic inertinite-rich coals of the Muli Coalfield on the Tibetan Plateau. *Int. J. Coal Geol.* **2015**, *144*, 23–47. [CrossRef]
75. Hayashi, K.I.; Fujisawa, H.; Holland, H.D.; Ohmoto, H. Geochemistry of ~1.9 Ga sedimentary rocks from northeastern Labrador, Canada. *Geochim. Cosmochim. Acta* **1997**, *21*, 4115–4137. [CrossRef]
76. Zheng, X.; Wang, Z.; Wang, L.; Xu, Y.; Liu, J. Mineralogical and Geochemical Compositions of the Lopingian Coals and Carbonaceous Rocks in the Shugentian Coalfield, Yunnan, China: With Emphasis on Fe-Bearing Minerals in a Continental-Marine Transitional Environment. *Minerals* **2017**, *7*, 170. [CrossRef]
77. Dai, S.; Yang, J.; Ward, C.R.; Hower, J.C.; Liu, H.; Garrison, T.M.; French, D.; O'Keefe, J.M.K. Geochemical and mineralogical evidence for a coal-hosted uranium deposit in the Yili Basin, Xinjiang, northwestern China. *Ore Geol. Rev.* **2015**, *70*, 1–30. [CrossRef]
78. Qi, H.; Hu, R.; Zhang, Q. REE Geochemistry of the Cretaceous lignite from Wulantuga Germanium Deposit, Inner Mongolia, Northeastern China. *Int. J. Coal Geol.* **2007**, *71*, 329–344. [CrossRef]
79. Bau, M.; Schmidt, K.; Koschinsky, A.; Hein, J.; Kuhn, T.; Usui, A. Discriminating between different genetic types of marine ferro-manganese crusts and nodules based on rare earth elements and yttrium. *Chem. Geol.* **2014**, *381*, 1–9. [CrossRef]
80. Michard, A.; Albarède, F. The REE content of some hydrothermal fluids. *Chem. Geol.* **1986**, *55*, 51–60. [CrossRef]
81. Dai, S.; Guo, W.; Nechaev, V.P.; French, D.; Ward, C.R.; Spiro, B.F.; Finkelman, R.B. Modes of occurrence and origin of mineral matter in the Palaeogene coal (No. 19-2) from the Hunchun Coalfield, Jilin Province, China. *Int. J. Coal Geol.* **2018**. [CrossRef]
82. Dai, S.; Zheng, X.; Wang, X.; Finkelman, R.B.; Jiang, Y.; Ren, D.; Yan, X.; Zhou, Y. Stone coal in China: A review. *Int. Geol. Rev.* **2017**. [CrossRef]

83. Dai, S.; Liu, J.; Ward, C.R.; Hower, J.C.; French, D.; Jia, S.; Hood, M.M.; Garrison, T.M. Mineralogical and geochemical compositions of Late Permian coals and host rocks from the Guxu Coalfield, Sichuan Province, China, with emphasis on enrichment of rare metals. *Int. J. Coal Geol.* **2016**, *166*, 71–95. [CrossRef]
84. Dai, S.; Zhang, W.; Ward, C.R.; Seredin, V.V.; Hower, J.C.; Li, X.; Song, W.; Wang, X.; Kang, H.; Zheng, L.; et al. Mineralogical and geochemical anomalies of Late Permian coals from the Fusui Coalfield, Guangxi Province, southern China: Influences of terrigenous materials and hydrothermal fluids. *Int. J. Coal Geol.* **2013**, *105*, 60–84. [CrossRef]
85. Dai, S.; Zhang, W.; Seredin, V.V.; Ward, C.R.; Hower, J.C.; Song, W.; Wang, X.; Li, X.; Zhao, L.; Kang, H.; et al. Factors controlling geochemical and mineralogical compositions of coals preserved within marine carbonate successions: A case study from the Heshan Coalfield, southern China. *Int. J. Coal Geol.* **2013**, *109*, 77–100. [CrossRef]
86. Ren, D.; Zhao, F.; Dai, S.; Zhang, J.; Luo, K. *Geochemistry of Trace Elements in Coal*; Science Press: Beijing, China, 2006; (In Chinese with an English abstract).
87. Zhou, Y.; Ren, Y. Distribution of arsenic in coals of Yunnan Province, China, and its controlling factors. *Int. J. Coal Geol.* **1992**, *20*, 85–98. [CrossRef]
88. Dai, S.; Wang, P.; Ward, C.R.; Tang, Y.; Song, X.; Jiang, J.; Hower, J.C.; Li, T.; Seredin, V.V.; Wagner, N.J.; et al. Elemental and mineralogical anomalies in the coal-hosted Ge ore deposit of Lincang, Yunnan, southwestern China: Key role of N_2–CO_2-mixed hydrothermal solutions. *Int. J. Coal Geol.* **2015**, *152*, 19–46. [CrossRef]
89. Zhao, L.; Ward, C.R.; French, D.; Graham, I.T.; Dai, S.; Yang, C.; Xie, P.; Zhang, S. Origin of a kaolinite-NH_4-illite-pyrophyllite-chlorite assemblage in a marine-influenced anthracite and associated strata from the Jincheng Coalfield, Qinshui Basin, Northern China. *Int. J. Coal Geol.* **2018**, *185*, 61–78. [CrossRef]
90. Etschmann, B.; Liu, W.; Li, K.; Dai, S.; Reith, F.; Falconer, D.; Kerr, G.; Paterson, D.; Howard, D.; Kappen, P.; et al. Enrichment of germanium and associated arsenic and tungsten in coal and roll-front uranium deposits. *Chem. Geol.* **2017**, *463*, 29–49. [CrossRef]
91. Zhao, L.; Dai, S.; Graham, I.; Wang, P. Clay mineralogy of coal-hosted Nb-Zr-REE-Ga mineralized beds from Late Permian strata, eastern Yunnan, SW China: Implications for palaeotemperature and origin of the micro-quartz. *Minerals* **2016**, *6*, 45. [CrossRef]
92. Dai, S.; Nechaev, V.P.; Chekryzhov, I.Y.; Zhao, L.; Vysotskiy, S.V.; Graham, I.; Ward, C.R.; Ignatiev, A.V.; Velivetskaya, T.A.; Zhao, L.; et al. A model for Nb–Zr–REE–Ga enrichment in Lopingian altered alkaline volcanic ashes: Key evidence of H-O isotopes. *Lithos* **2018**. [CrossRef]
93. Zhao, L.; Zhu, Q.; Jia, S.; Zou, J.; Nechaev, V.; Dai, S. Origin of minerals and critical metals in an argillized tuff from the Huayingshan Coalfield, southwestern China. *Minerals* **2017**, *7*, 92. [CrossRef]
94. Dai, S.; Yan, X.; Ward, C.R.; Hower, J.C.; Zhao, L.; Wang, X.; Zhao, L.; Ren, D.; Finkelman, R.B. Valuable elements in Chinese coals: A review. *Int. Geol. Rev.* **2016**. [CrossRef]
95. Dai, S.; Zhou, Y.; Ren, D.; Wang, X.; Li, D.; Zhao, L. Geochemistry and mineralogy of the Late Permian coals from the Songzao Coalfield, Chongqing, southwestern China. *Sci. China Ser. D-Earth Sci.* **2007**, *50*, 678–688. [CrossRef]
96. Dai, S.; Wang, X.; Zhou, Y.; Hower, J.C.; Li, D.; Chen, W.; Zhu, X.; Zou, J. Chemical and mineralogical compositions of silicic, mafic, and alkali tonsteins in the late Permian coals from the Songzao Coalfield, Chongqing, Southwest China. *Chem. Geol.* **2011**, *282*, 29–44. [CrossRef]